BRAIN DYNAMICS AND MEMORY ENHANCEMENT: MEMRISTOR BASED MODELS

A Thesis Submitted to
the Graduate School of Engineering and Sciences of
İzmir Institute of Technology
in Partial Fulfillment of the Requirements for the Degree of

MASTER OF SCIENCE

in Electronics and Communication Engineering

by
Ufuk YÜCEL

July 2014
İZMİR

We approve the thesis of **Ufuk YÜCEL**

Prof. Dr. F. Acar SAVACI
Department of Electrical and Electronics Engineering,
İzmir Institute of Technology

Prof. Dr. Bilge KARAÇALI
Department of Electrical and Electronics Engineering,
İzmir Institute of Technology

Prof. Dr. Nejat BULUT
Department of Physics,
İzmir Institute of Technology

22 July 2014

Prof. Dr. F. Acar SAVACI
Supervisor
Department of Electrical and Electronics Engineering,
İzmir Institute of Technology

Prof. Dr. M. Salih DİNLEYİCİ
Head of the Department of
Electrical and Electronics Engineering

Prof. Dr. R. Tuğrul SENGER
Dean of the Graduate School of
Engineering and Sciences

ACKNOWLEDGEMENTS

I would like to express my gratitude to my supervisor Prof. Dr. F. Acar SAVACI for his scientific guidance, support and motivation during this study and preparation of this thesis. I would also like to express my gratitude to my committee member Prof. Dr. Nejat BULUT and Prof. Dr. Bilge KARAÇALI for their contributions.

ABSTRACT

BRAIN DYNAMICS AND MEMORY ENHANCEMENT: MEMRISTOR BASED MODELS

In this thesis, the memory systems of the brain are researched and the relationship between these memory systems and memristor theory are studied. Firstly, the ideal memristor theory is studied. By using the cubic memristor that was based on the ideal memristor theory, the basic logical operations are explained. Additionally, the nerve cells and synapses, which are thought where the memory and learning take place, are inquired. Bearing in mind that the characteristic of the memristor and its similarities between the synapses has been researched with the previous studies on this field. Finally, memristor data storage system has been designed by using memristors, and a binary image of 12x60 pixels has been successfully stored on this design. Also, the edge detection for images has been presented by using the memristor cellular automaton and some examples have also been given.

ÖZET

BEYİN DİNAMİĞİ VE BELLEK GÜÇLENDİRİLMESİ: MEMRİSTÖR TABANLI MODELLER

Bu tezde, beynin hafıza olgusu incelenmiş ve memristor teorisi ile olan ilişkileri araştırılmışır. İlk olarak, ideal memristor modeli incelenmiştir. Bu modelden yola çıkarak oluşturulmuş olan kübik memristor kullanılarak, basit mantık operasyonları anlatılmıştır. Daha sonra, hafıza ve öğrenmenin gerçekleştiği sinapslar incelenmiştir. İncelenen memristör karakteristiği ile birlikte, memristorün gösterdiği davranışların sinapslar ile olan benzerliği ve bu konu üzerine yapılan çalışmalar aktarılmıştır. Son olarak, memristör karakteristiğinden faydalanılarak, memristor bilgi depolama sistemi tasarlanmış ve bu sisteme 12x60 lık bir resim kaydetme işlemi uygulanmıştır. Ayrıca, resimlerdeki kenarları detekte eden bir memristive sistem anlatılmış ve bazı örnekler verilmiştir.

TABLE OF CONTENTS

LIST OF FIGURES

Figure **Page**

LIST OF TABLES

Table **Page**

CHAPTER 1

INTRODUCTION

In 1971, Leon O. Chua presented a new two-terminal circuit element characterized by the charge and flux-linkage (Chua, 1971). He named this new element 'Memristor-Memory Resistor' as the fourth new basic circuit element. Chua has been influenced by Mendeleev's periodic table of chemical elements in nature (Mendeleev, 1897). Once Mendeleev had completed his periodic table, he noticed that there were some missing chemical elements on his periodic table. His hypothesis claimed that these elements must exist. This hypothesis depended on the relationship between the properties of the closest elements with the missing element. With this idea, Chua started to think about three fundamental circuit elements and their relationships with each other based on the symmetry arguments. He finally noticed a missing element, which appeared due to the relationship between magnetic flux-linkage and charge. In Figure 1.1, the diagram presents the six possible relations. These possible relations are the relations between voltage V, current i, charge q and flux ψ. The four fundamental two-terminal passive circuit elements give four relations. The relationship between the voltage and current gives the resistor R, the relationship between the charge and voltage gives the capacitor C, the relationship between the flux and current gives the inductor L and finally the relationship between the charge and flux gives the memristor M.

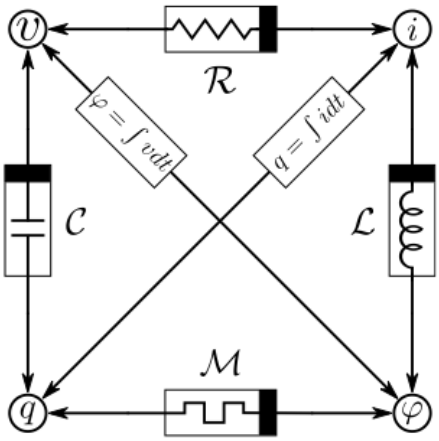

Figure 1.1: The symmetry arguments between the resistor, capacitor, inductor and memristor(Iu.H, 2013)

On the contrary of the traditional resistances, the electrical resistance of memristor is not constant. Its resistance depends on the current that have flown through the device. It means that the memristor remembers its history and does not require any power supply to keep its resistance unchanged (Chua, 2011).

The memristor still has unique properties that cannot be exhibited by a resistor, capacitor or inductor. 37 years before 2008, Chua implied that memristor was not discovered as a physical device without internal power supply, but he implied its importance for its application areas. The HP Group, from the USA, declared that they found the memristor as a physical device by using TiO_2 thin film (Strukov, et al. 2008). It was the first nanoscale solid-state device recognized as a memristor.

After HP announced that the missing memristor was found, the interest of both scientific researches and electronic industry has been reignited. This interest comes from the unique properties of the memristor such as nanoscale size, low-power consumption, nonvolatile memory, and synapse-like behavior.

Memristors are convenient to use in the digital computing areas. These types of applications are based on a programmable memristor acting as a switch. This switch is configured to the two resistance levels. These levels are accredited one of the two logical values (0 and 1) and these devices are used as a binary switch, which can present outcomes of Boolean functions. In future computer engineering, memristor will play an important role in the Resistive random-access memory (RRAM) applications (Xu, et al. 2011). Developing the memristor technology helps the RRAM applications with the digital memory applications. RRAM creates different layers of electrical resistance to store the information by using ions. The traditional methods use bits to store the

information, while RRAM uses the high resistance level or low resistance level to make up bits of information. Due to the fact that RRAM is non-volatile, the memristor could possibly be used in RRAM applications. RRAM applications of the memristor open an access to store big data on the dimension of nanometers. Some companies such as Panasonic, Rambus and HP have been working on the RRAM technologies and patented their works. To achieve the computational ability of brain it is required the invention of small and cheap circuit elements that mimic these synapses (Snider, 2008). Snider with the HP Group then announced their experimental results of CMOS architecture. Their memristive nanodevices give the opportunity to work with densities greater than 10^{10} devices per cm^2. A Wheatstone-bridge like circuit composed of memristors has been also described (Hyongsuk, et al. 2012). This circuit proposed a relationship between the synaptic weight and synaptic input signal.

On the contrary of digital applications of the memristor, analog applications have attracted so much attention. One of the most important analog applications is the bio-inspired circuits. These circuits perform a particular task of a biological neural network. These biological neural networks are inspired from the human or animal's neural systems. In human brain, neurons operate the incoming signals and transmit signals to other neurons through synapses. The incoming signals multiplied by the synapse weight and the synapse readjusts its weight by a nonlinear function. This function depends on the history of the input signal. Memristors are convenient elements for this functionality of the synapses. In human brain there are 10^6 neurons per cm^2. This high ratio of the synapses in the brain precludes the implementation of the synaptic functionality by using conventional transistors. Since memristors are the nanoscale devices, they can be used instead of the conventional transistors. The first mathematical model that describes how the information flows through the neurons are presented by Alan Lloyd Hodgkin and Andrew Huxley. Their model describes the action potential of giant squid axon (Hodgkin-Huxley, 1952). They composed a set of nonlinear differential equations that models the electrical characteristic of neurons. It describes the ionic mechanism for propagation and initiation in the squid giant axon. Bailey and Kandel pointed out that the biology of memory in brain occurs after some physical changes (Kandel-Craig, 1993). They also thought the stability of the memory in long-term period was because of the stability of synaptic modifications. Caporale and Dan, focused on the Spike Timing-Dependent Plasticity, STDP (Natalia-Dan, 2008). They considered two points that STDP is based on its dendritic location in brain and complex

input trains that modulate the STDP. Snider with Information and Quantum Systems Laboratory implemented timing-based learning rules known as STDP (Greg, 2008). They pointed out some reasons why the neuromorphic circuits such as massive parallelism, are attractive. Because of the natural nonlinear characteristics of memristor, it is used to model some biological organisms or biological facts. DiVentra *et.al*. models amoeba learning in which amoeba exists under some special conditions (Di Ventra, et al. 2009). Pershin and diVentra described an artificial synapse that remembers its history and it should be plastic according to the pre-synaptic and post-synaptic neuronal activities (Di Ventra-Pershin, 2010). These types of activities are related to the associative memory. Hyun Jo, et.al. experimentally showed that a silicon-based memristor device that presents the characteristics of biological synapses such as STDP (Hyun, et al. 2010). Takeo Ohno *et.al*. formed an Ag_2S inorganic synapse that presents the characteristics of biological synapses (Takeo, et al. 2011). Their inorganic synapse implemented short-term plasticity and long-term potentiating properties in brain. S. G. Hu, *et.al*. experimentally formed a NiO-based memristor that emulates the forgetting curve of the human brain (Hu, et al. 2013). In this work, memristor conductance corresponds to learning or forgetting events, which occurred in biological synapses, and results that showed similar characteristics of Ebbinghaus forgetting curves.

1.1 Outline of the thesis

This thesis is structured as follows:

Chapter 1: Introduction

This chapter introduces how the memristor was found. It also introduces the application areas of the memristors.

Chapter 2: The Memristor

In this chapter, memristor characteristic equations have been obtained and it has been explained why memristors can be used as memory storage elements. Some basic logical operations by memristors have been presented.

Chapter 3: Synaptic Plasticity

In this chapter, synaptic modifications for the long term and short term potentiation and learning events in the brain have been presented. Then it has been explained why memristors are convenient to use in bio-inspired applications.

Chapter 4: Memristive Storage System

In this chapter, a memristive crossbar array has been presented. These arrays are connected by memristors and they are convenient to store logical values such as logic ‘1’ and logic ‘0’. Also, the edge detection for images has been introduced by using memristor cellular automata.

Chapter 5: Conclusion

This chapter summarizes the memristor theory and applications introduced in this thesis.

CHAPTER 2

THE MEMRISTOR

A memristor is characterized by the constitutive relation $f_M(\psi, q) = 0$ relating the charge 'q' and the flux 'ψ'. The charge and flux are given by

$$q(t) = \int_{-\infty}^{t} i(\tau)d\tau = q_0 + \int_{0}^{t} i(\tau)d\tau \tag{2.1}$$

$$\psi(t) = \int_{-\infty}^{t} V(\tau)d\tau = \psi_0 + \int_{0}^{t} V(\tau)d\tau \tag{2.2}$$

Here q_0 and ψ_0 are the initial charge and flux at t=0. More simply, the input-output response of a memristor is determined by the charge-flux curve. It is classified as ideal if the charge-flux curve is unique, continuously differentiable and monotonically increasing. If the memristor constitutive relation is described as an explicit function of q or ψ, it is called the charge-controlled memristor or flux-controlled memristor, respectively.

$$\psi = \hat{\psi}(q) \;\; for\ the\ charge - controlled \tag{2.3}$$

$$q = \hat{q}(\psi)\ for\ the\ flux - controlled \tag{2.4}$$

Differentiating Equation 2.3 and 2.4 with respect to time, it is obtained as

$$V = \frac{d\psi}{dt} = \frac{d\hat{\psi}(q)}{dq}\frac{dq}{dt} = M(q)i\ for\ the\ charge\ controlled, \tag{2.5}$$

$$\frac{dq}{dt} = \frac{d\hat{q}(\psi)}{d\psi}\frac{d\psi}{dt} \;\; for\ the\ flux - controlled \tag{2.6}$$

where $d\psi/dt = V$ and $dq/dt = i$. For the charge-controlled case, the Equation 2.5 is given by

$$V = M(q)i(t) \tag{2.7}$$

where $M(q) = d\hat{\psi}(q)/dq$ is the memristance measured in Ohms (Ω). The memristance corresponds to the slope of the $q - \psi$ curve. Similarly, for the flux-controlled case, the Equation 2.6 is given by

$$i = W(\psi)V(t) \tag{2.8}$$

where $W(\psi) = d\hat{q}(\psi)/d\psi$ is the memductance measured in Siemens (S). The memductance corresponds to the slope of the $\psi - q$ curve.

Chua suggested a theorem called as the passivity criterion that shows what class of memristors might be discovered without internal power supplies (Chua, 1971).

Theorem 2.1: The Passivity Criterion

A memristor characterized by a differentiable $(q - \psi)$ *curve is passive if, and only if, its memristance* $M(q) \geq 0$ *at any instant of time.*

The instantaneous power dissipated by a memristor is

$$p(t) = V(t)i(t) = M\big(q(t)\big)[i(t)]^2 \tag{2.9}$$

If the memristance $\mathrm{M(q)} \geq 0$, then $p(t) \geq 0$, and the memristor is passive. This theorem determines the properties of the $(\psi - \mathrm{q})$ curve so that the memristor is passive (without internal power supplies). If there exists a point q_0 such that $M(q_0) < 0$. The differentiability of the $(\mathrm{q} - \psi)$ curve implies that there exists an $\epsilon > 0$ such that

$M(q_0 + \Delta q) < 0$, $|\Delta q| < \epsilon$. Then memristor is driven by a current i(t), which is zero for t<t' and such that

$$q(t) = q_0 + \Delta q(t) \;\; for \;\; t' \leq t_0 \leq t \;\; ; \;\; |\Delta q(t)| < \epsilon. \tag{2.10}$$

Then it is obtained that the memristor is active since

$$\int_{-\infty}^{t} P(\tau) d\tau < 0. \tag{2.11}$$

It is clear that if the memristor is characterized by a monotonically increasing $(\psi - q)$ curve, the memristor can exist in a device form without internal power supplies.

In Equations 2.7 and 2.8, the memristance and memductance depend on the history of the input. The memristance or memductance is a function of q and ψ. Replacing q in 2.7 with 2.1 and ψ in 2.8 with 2.2 gives

$$V(t) = M\{\int_{-\infty}^{t} i(\tau) d\tau\} i(t) \tag{2.12}$$

and

$$i(t) = W\{\int_{-\infty}^{t} V(\tau) d\tau\} V(t) \tag{2.13}$$

The entire past history of the input signal determines the memristance or memductance. After the input signal is shut down, the memristor keeps the memristance value or memductance value indefinitely.

2.1. Non-Volatile Memory Criteria

A memristor obeys the state-dependent Ohm's law when the current i(t) is the input:

1- Current controlled state-dependent Ohm's law:

$$V = R(\boldsymbol{x}) i \tag{2.14}$$

$$\frac{d\boldsymbol{x}}{dt} = f(\boldsymbol{x}, i) \tag{2.15}$$

where **x** denotes a vector with n internal state variables.

2- When the voltage V(t) is the input, the voltage-controlled state-dependent Ohm's law

$$i = G(\boldsymbol{x})V \tag{2.16}$$

$$\frac{d\boldsymbol{x}}{dt} = g(\boldsymbol{x}, V) \tag{2.17}$$

By following these definitions, a memristor has non-volatile memory if and only if

$$f(\boldsymbol{x}, i) = 0 \; whenever \; i = 0 \; for \; all \; \boldsymbol{x} \in \mathbb{R}^n \tag{2.18}$$

or

$$g(\boldsymbol{x}, V) = 0 \; whenever \; V = 0 \; for \; all \; \boldsymbol{x} \in \mathbb{R}^n \tag{2.19}$$

When the power supply is shut down (V = 0), $\frac{d\boldsymbol{x}}{dt} = f(\boldsymbol{x}, 0) = 0$ for all $\mathbf{x} \in \mathbb{R}^n$ and $\mathbf{x} \in \mathbb{R}^n$ is an equilibrium state of a memristor.

$q - \psi$ curve of an ideal memristor:

It has been mentioned that $q - \psi$ curve of a memristor should be unique, continuously differentiable and monotonically increasing. It should be unique because the memristor should respond in the same way when it is driven by any kind of waveform. It means that a certain amount of charge or flux changes the memristance or memductance in a same way. It should be continuously differentiable because the slope of the curve, memristance, is uniquely defined at every point and it is finite. It should also be monotonically increasing because the memristance is positive in order to guarantee passivity. Additionally, $q - \psi$ curve of an ideal memristor should be a one-to-one function because from Equation 2.7 and 2.8, it is obtained that $M(q) = {}^{1}/_{W(\psi)}$.

For an example, a $q-\psi$ curve is defined in Equation 2.20 and shown in Figure 2.1. It satisfies the criteria of unique, continuously differentiable and monotonically increasing (Chua, 2011).

$$\varphi = q + {}^{1}/_{3}\, q^{3} \tag{2.20}$$

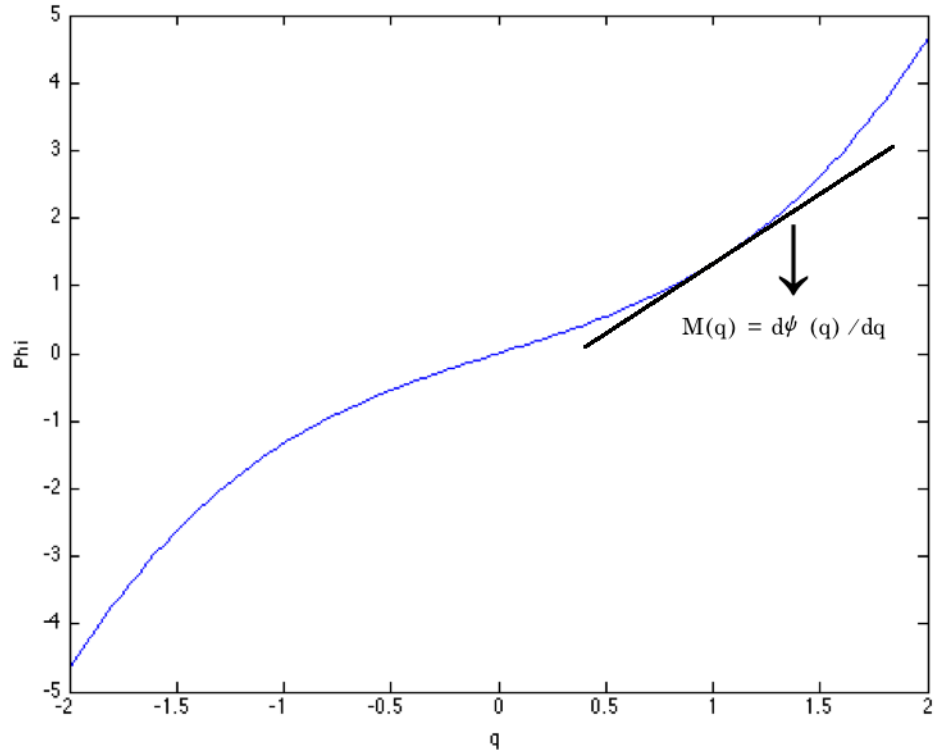

Figure 2.1: The cubic memristor q- φ characteristic

The slope of the $q-\psi$ curve gives the memristance $M(q) = {}^{d\psi(q)}/_{dq}$ and it is shown in Figure 2.1. For this type of cubic memristor, the relationship between the applied current and voltage across the memristor gives a hysteresis. A sinusoidal current waveform is applied as

$$i(t) = \begin{cases} Asin(wt), & t \geq 0 \\ 0, & t < 0 \end{cases} \tag{2.21}$$

The charge on the memristor from Equation 2.1 gives

$$q(t) = \int_0^t Asin(w\tau)d\tau = \frac{A}{w}(1 - coswt)\ ;\ t \geq 0 \tag{2.21}$$

and the flux-linkage of the memristor is

$$\varphi = q + {}^1\!/_3\, q^3 \Rightarrow\ \varphi(t) = \frac{A}{w}(1 - coswt)\{1 + \frac{1}{3}\left(\frac{A^2}{w^2}\right)(1 - coswt)^2\} \tag{2.22}$$

The voltage across the memristor is obtained as

$$\frac{d\varphi}{dt} = V(t) = A\{1 + \frac{A^2}{w^2}(1 - coswt)^2\}sinwt \tag{2.23}$$

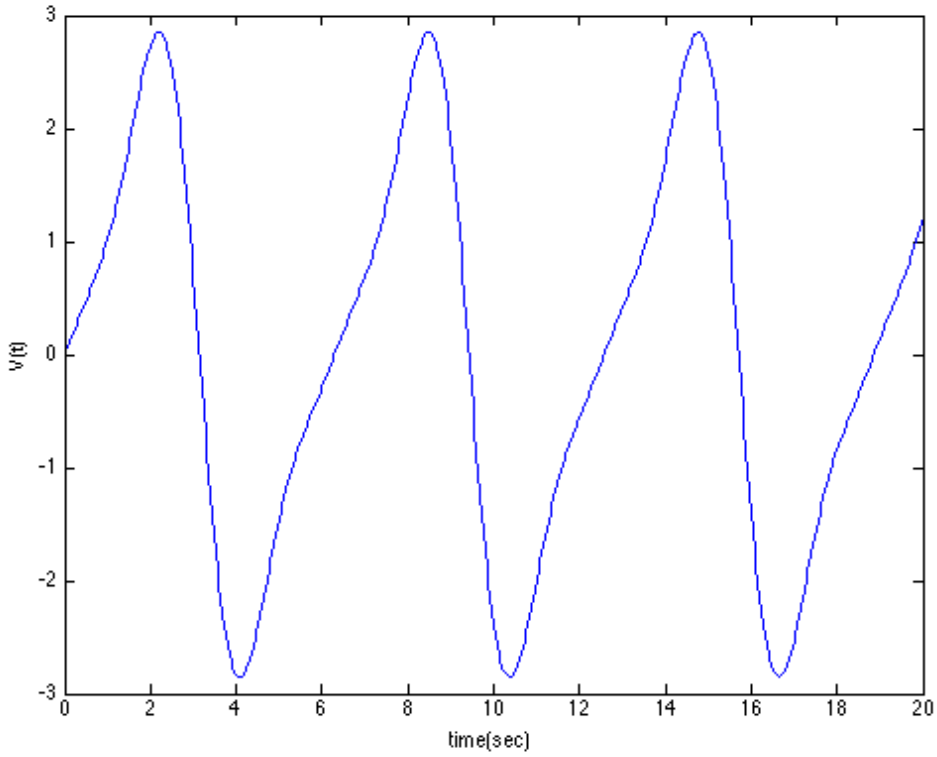

Figure 2.2: Cubic memristor voltage vs. time loci

To sum up, the applied current and the voltage on the cubic memristor are

$$i(t) = Asin(wt)\ ;t \geq 0 \tag{2.24}$$

and

$$V(t) = A\{1 + \frac{A^2}{w^2}(1 - coswt)^2\}sinwt \tag{2.25}$$

If these functions i(t) and V(t) are plotted on MATLAB platform, the pinched-hysteresis loop is obtained. The hysteresis occurs because i(t) and V(t) will be zero at the same time and they do not reach their maximum values at the same time. When a memristor is driven by a periodic voltage or current source, it exhibits the pinched hysteresis loop of the v-i loci. For each of periods these sources span both positive and negative values. It is important that this characterization identifies a device under applied periodic input signals shows a pinched hysteresis loop. A passive memristor driven by a sinusoidal excitation always shows hysteretic i-v response crossing the origin. The area of this loop depends on the frequency or the amplitude of the input waveform. When the frequency is increased while the amplitude is constant, the area of the hysteresis decreases because w is increased. When the amplitude is increased while the frequency is constant, the area of the hysteresis increases. The amplitude and frequency dependents are shown in Figure 2.3, 2.4, 2.5, and 2.6. In Figure 2.3, the amplitude of the input signal A is 1V when the frequency w is $1s^{-1}$. In Figure 2.4, the amplitude of the input signal A is 2V when the frequency w is $1s^{-1}$. In Figure 2.5, the amplitude of the input signal A is 1V when the frequency w is $2s^{-1}$. In Figure 2.6, the amplitude of the input signal A is 2V when the frequency w is $2s^{-1}$.

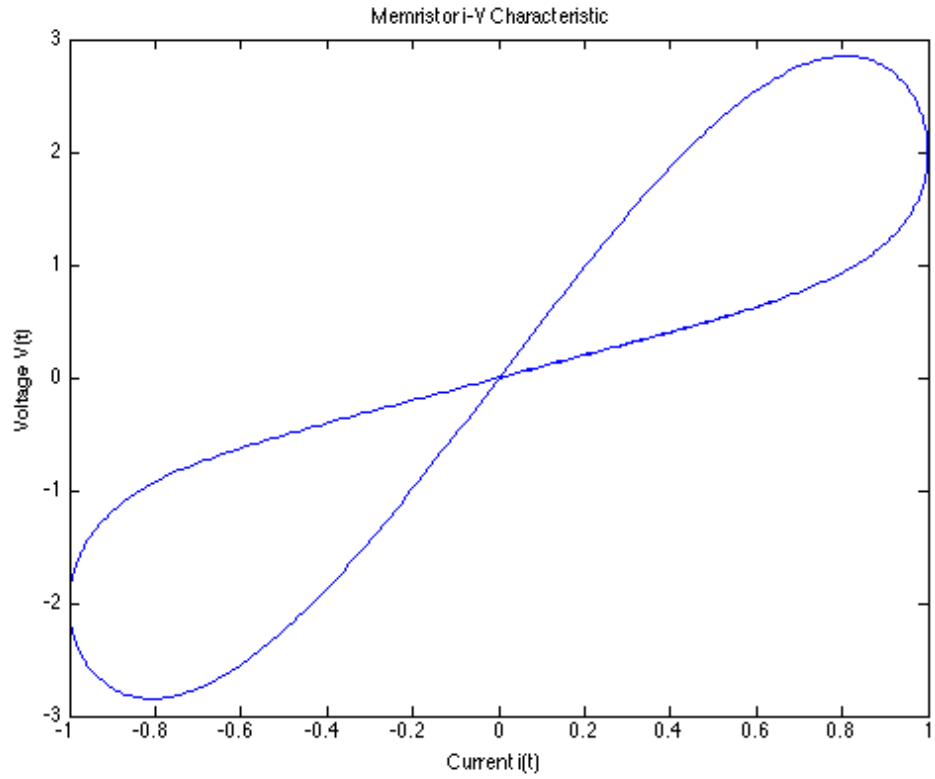

Figure 2.3: The amplitude of the input signal A=1V, the frequency w=1s^{-1}.

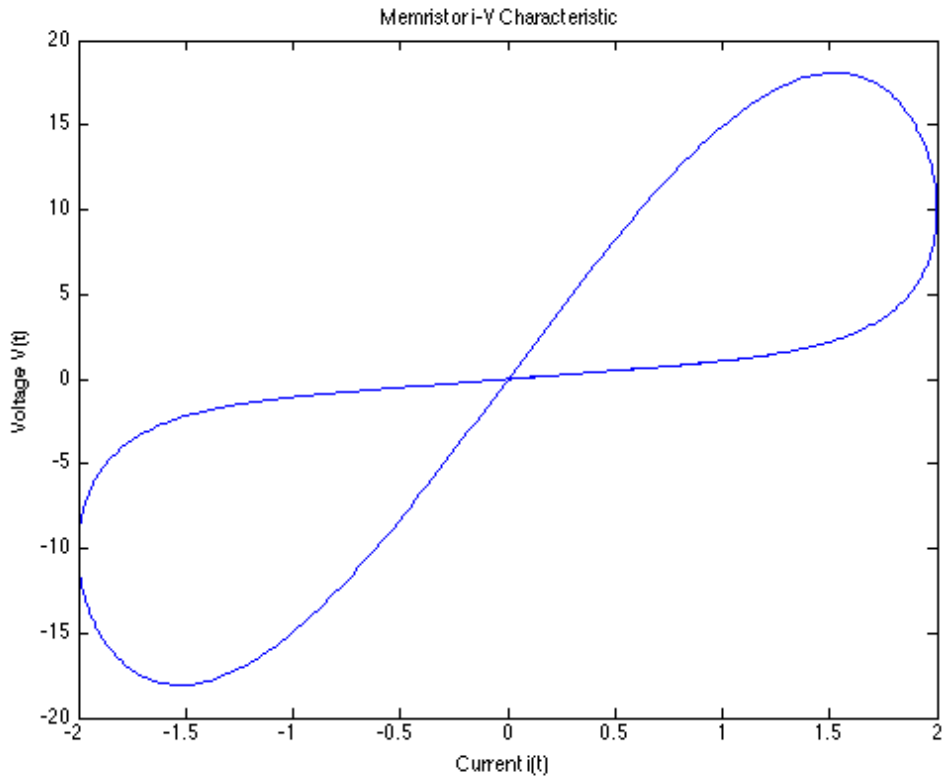

Figure 2.4: The amplitude of the input signal A=2V, the frequency w=1s^{-1}.

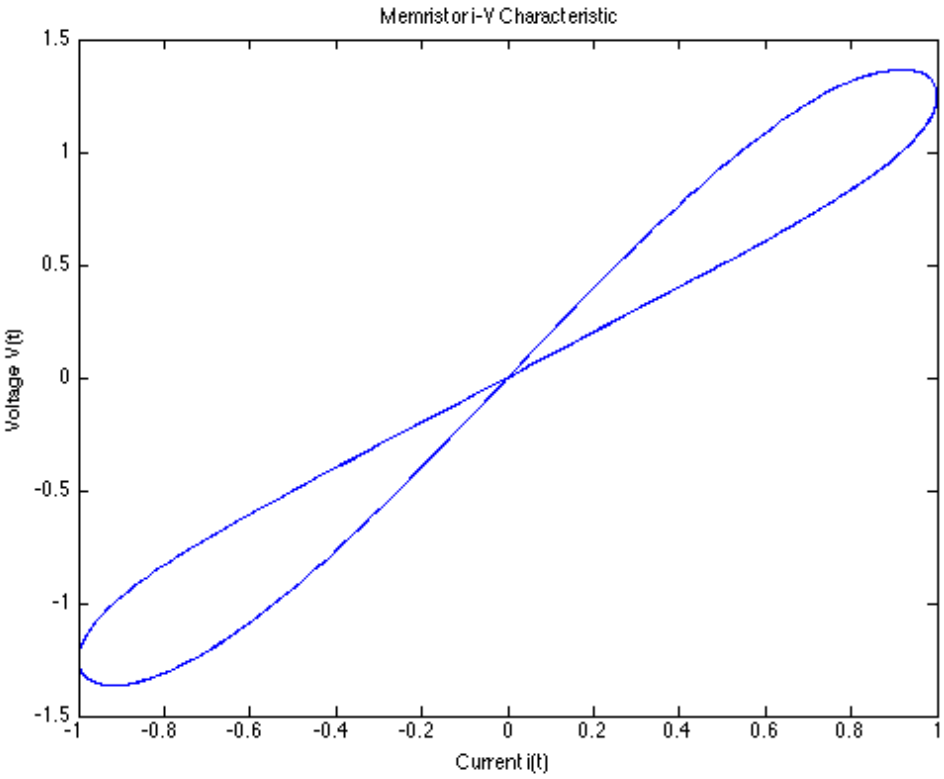

Figure 2.5: The amplitude of the input signal A=1V, the frequency w=2 s^{-1}.

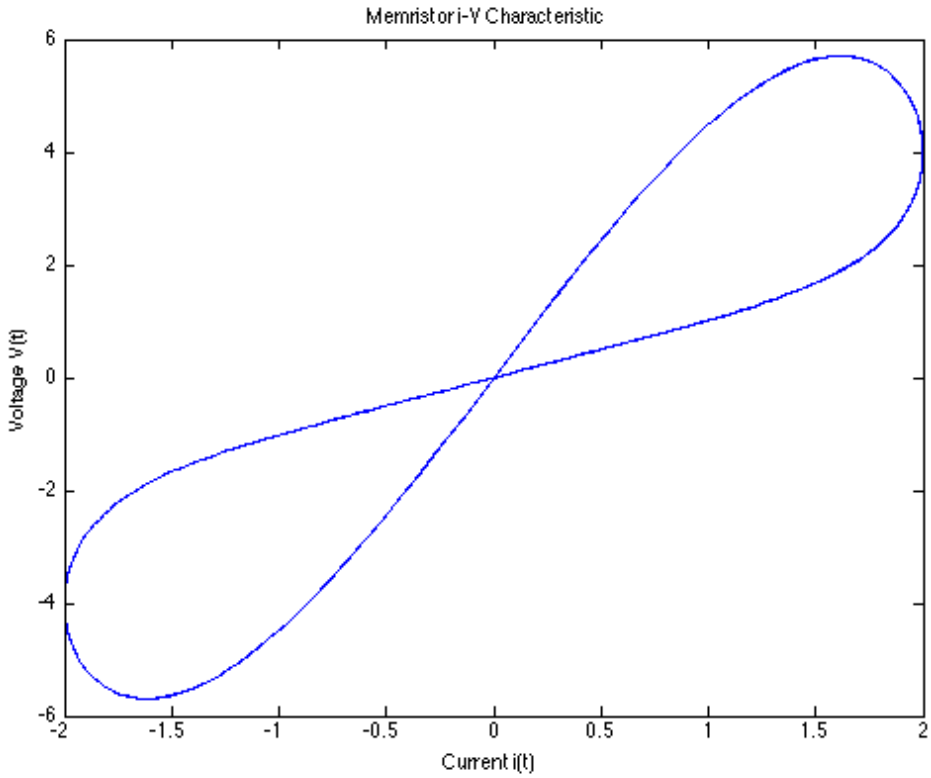

Figure 2.6: The amplitude of the input signal A=1V, the frequency w=1s^{-1}

The memristance ‘R’ of the memristor, the current ‘i’ through the memristor, the voltage ‘V’ across the memristor and the charge ‘q’ on the memristor are given in Figure 2.7.

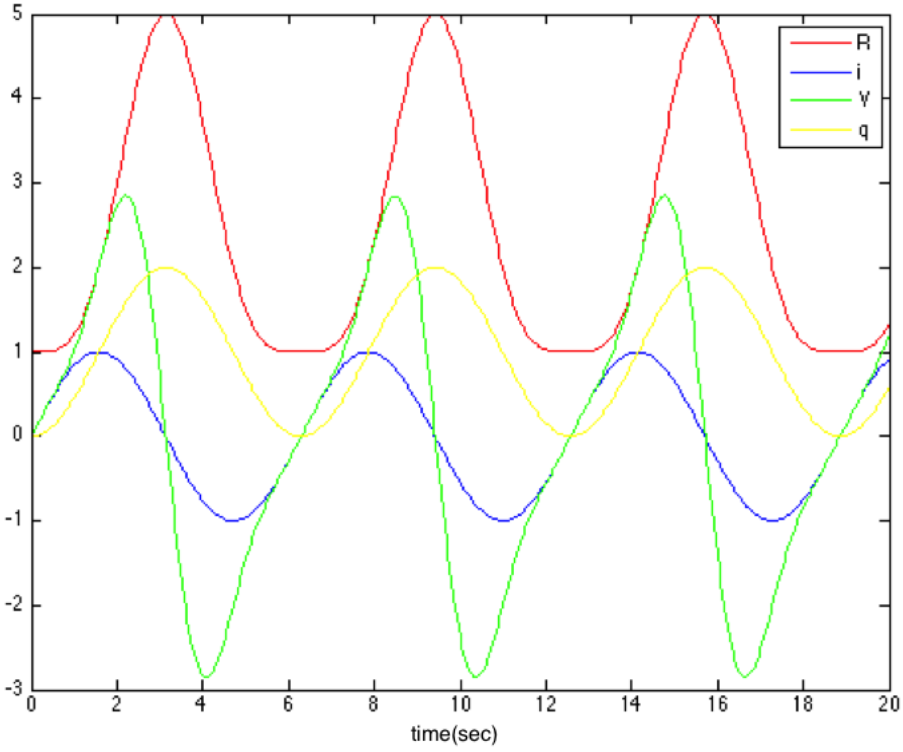

Figure 2.7: Memristance vs. time, current vs. time, voltage vs. time and charge vs. time for the cubic memristor

It is important to notice that the voltage and current are zero at the same time and the charge never has the value of zero.

2.3 HP Memristor

The HP-Group, USA, announced that the memristor was physically found in 2008 (Strukov, et al. 2008). Their invention of memristor architecture was based on a thin film, titanium dioxide (Ti is for titanium and O is for oxygen). The characteristic equations of this kind of memristor depend on how the moving process acts upon the memristive system. The memristor remembers the last memristance state even if the

power supply is turned off. One of the two TiO_2 layers consists of a perfect $^2/_1$ O_2 to Ti ratio. This ratio turns the memristor into an insulator and it is called as an undoped region. The other one has lost some O_2 and it is called the doped region and shown as TiO_{2-x} . This region makes the memristor conductive. When an external excitation, which is a periodic sinusoidal excitation, in general, is applied, it causes the charge dopants to drift. As a result the doped and undoped regions are not constant and they change the total memristance of the memristor. In Figure 2.8 the HP memristor doped and undoped regions are shown.

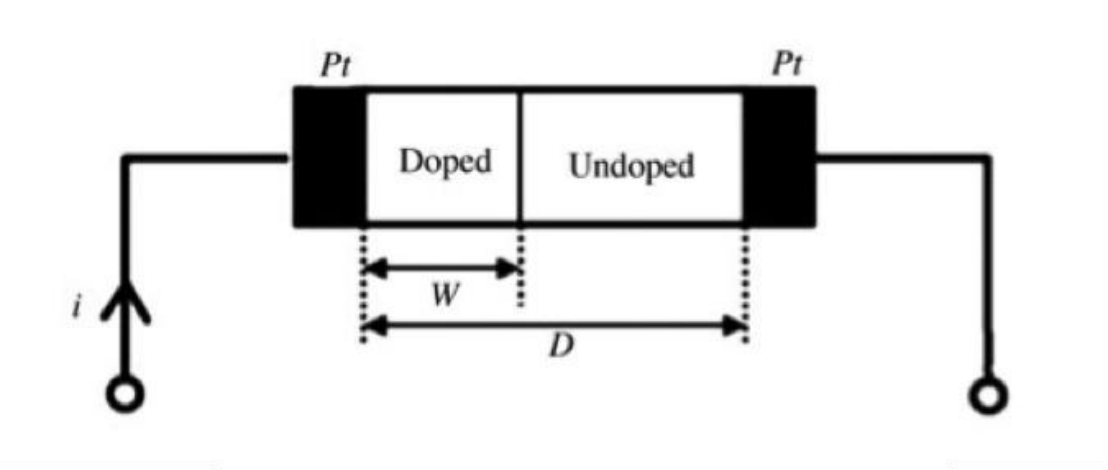

Figure 2.8: The HP memristor (Iu H. 2013).

'w' is the length of the doped region and 'D' is the total length. To increase W (decreases memristance), the positive bias should be applied. To decrease W (increases memristance), the negative bias should be applied to the memristor. In this model, the memristance is described by

$$R_{mem}(x) = R_{ON}x + R_{off}(1 - x) \qquad (2.26)$$

here $x = {}^W/_D \in (0, 1)$ and it is described as the internal state variables (Chua, 2011). As it has been described above, for W = 0, the final resistance value is described as R_{off} means that the highest memristance value and for W = D, the limit resistance value is described as R_{on} means that the lowest resistance value.

Ohm's law for a memristor is described as

$$V(t) = R_{mem}(x)i(t) \tag{2.27}$$

The HP memristor has a boundary between the doped region and undoped region and it is necessary to describe the motion of this boundary. The speed of this boundary motion depends on the doped region, the thickness of layers and the current that flows through the memristor. Mathematically, the state variables can be described as

$$\frac{dx}{dt} = ki(t) \tag{2.28}$$

where

$$k = \frac{\mu_V R_{on}}{D} \tag{2.29}$$

and the average ion mobility $\mu_V = 10^{-14} m^2 s^{-1} V^{-1}$. After integrating the Equation 2.28 the state variable x(t) can be obtained as

$$x(t) = \mu_V \frac{R_{on}}{D} q(t) \tag{2.30}$$

The voltage across the memristor $V(t) = R_{mem}(x)i(t)$ is as follows

$$V(t) = \left(R_{on} \frac{x(t)}{D} + R_{off} \left(1 - \frac{w(t)}{D} \right) \right) i(t). \tag{2.31}$$

As it can be understood from the Equation 2.28, 'k' is the ratio of the boundary speed to the current. For $R_{on} << R_{off}$ the memristance is formed as

$$M(q) = R_{off}(1 - \frac{\mu_V R_{on}}{D^2} q(t)) \tag{2.32}$$

For instance, the HP memristor is driven by a voltage source *V=sint* shown in Figure 2.9, the current through the memristor is obtained as Figure 2.10 given below. The i-v loci is then given in Figure 2.11.

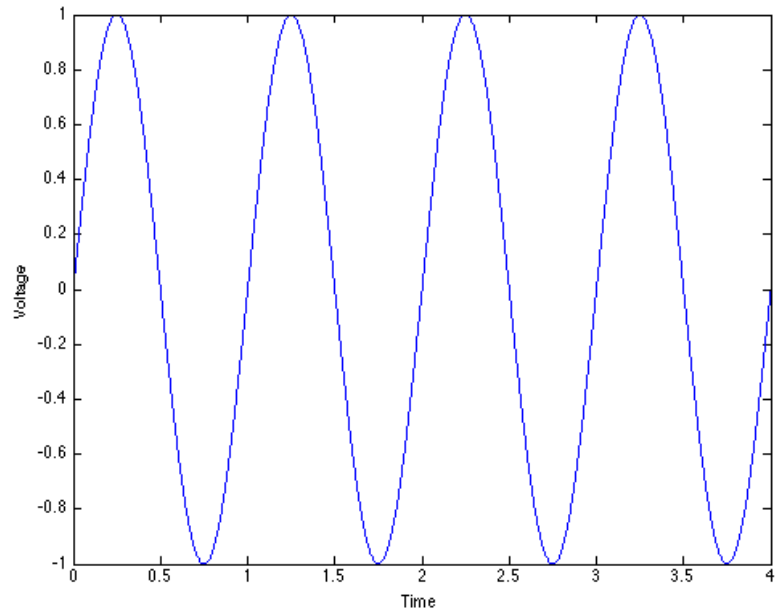

Figure 2.9: The Voltage vs. time loci of the memristor

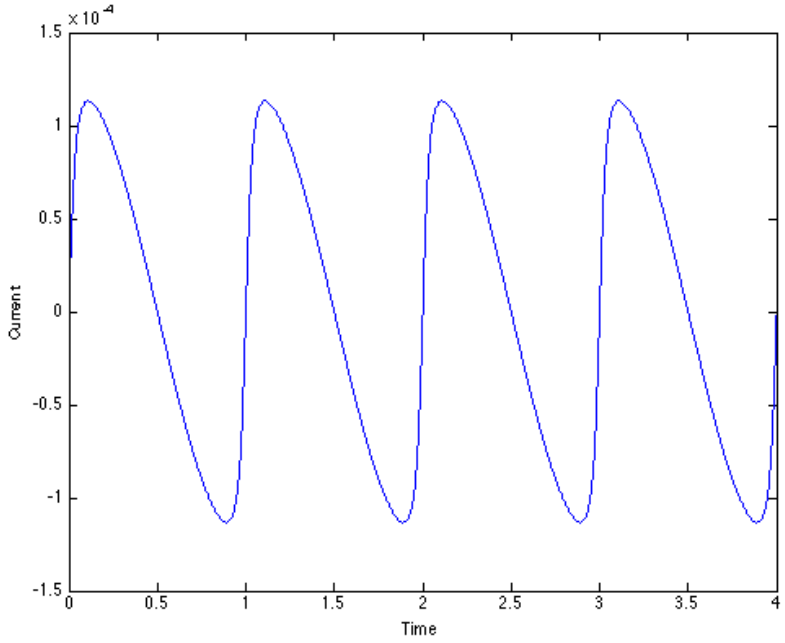

Figure 2.10: The current vs. time loci of the memristor

As it can be seen from the Figure 2.7, when the current reaches its maximum value at t=0.15s, the voltage does not reach its maximum value. In the Figure 11, these voltage and current changings give hysteresis loops.

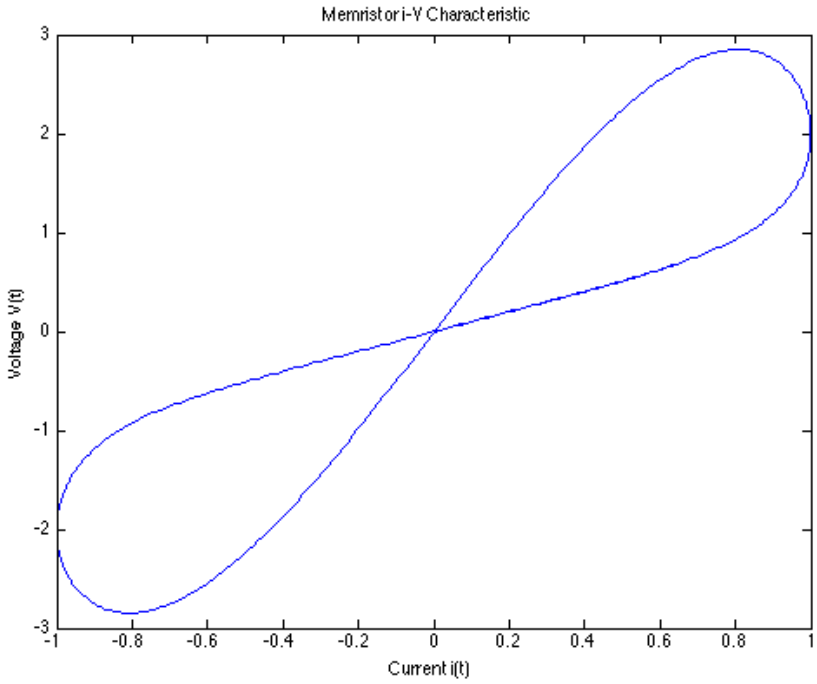

Figure 2.11: Memristor i-v loci

The memristance M(q) is given in Figure 2.12. The high resistance value is obtained as 15900Ω and the low resistance value is obtained as 2000Ω.

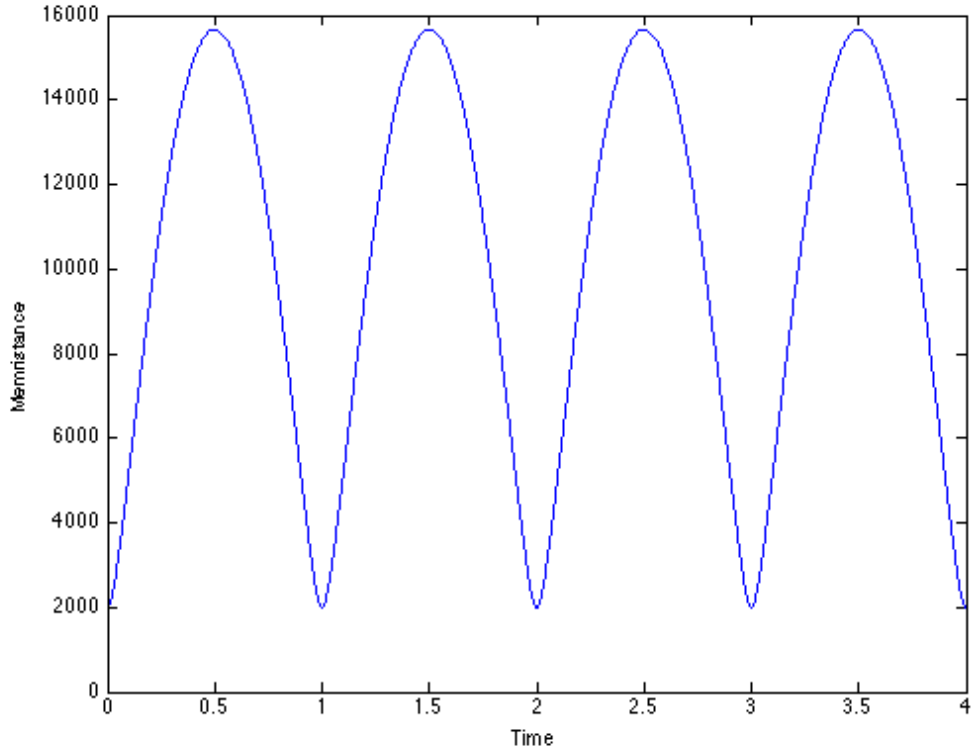

Figure 2.12: Memristance vs. time loci

In this memristor model all the dopants move linearly in the memristor. Due to the fact that a memristor is a nano-scale device, a large electric field can be occurred by a very small bias. This makes the dopants movement nonlinear. This nonlinearity can be very big at the boundaries of the memristor. For the actual memristor model, the nonlinear dopant drift model, it is necessary to add a window function to the linear dopant drift model.

$$\frac{dx}{dt} = ki(t)f(x) \tag{2.32}$$

Here the f(x) window function, called Joglekar window function, is described as

$$f(x) = 1 - (2x - 1)^{2p} \tag{2.33}$$

This Joglekar window function is plotted in Figure 2.13.

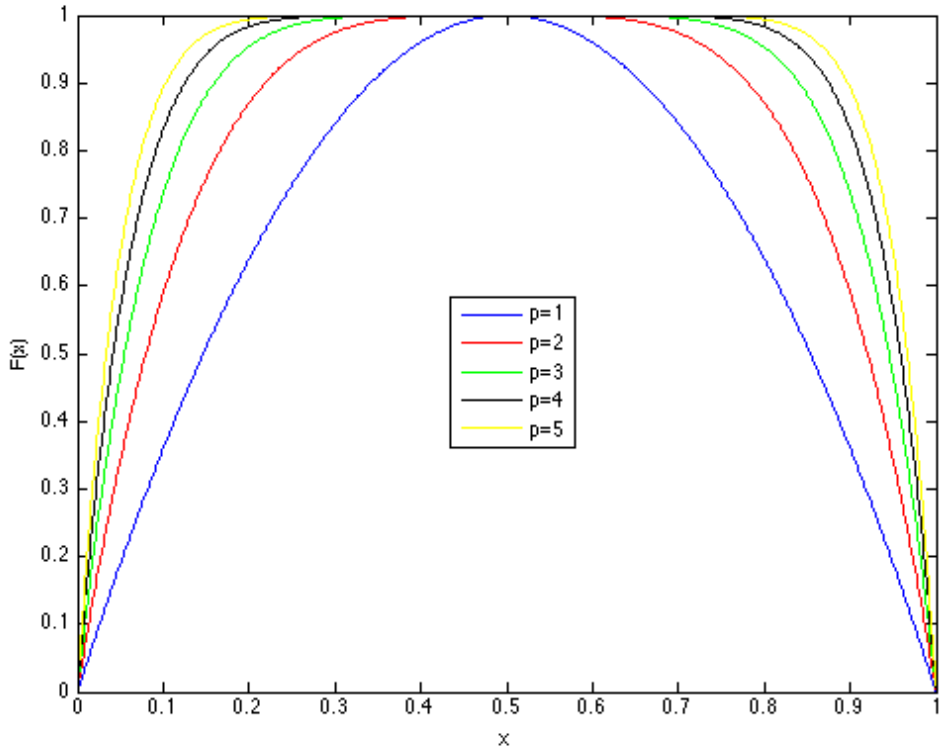

Figure 2.13: The window function for different values of ‘p’.

2.4. Memristor Bridge Synapses

Leon O. Chua described a Wheatstone-bridge like circuit composed of memristors (Hyongsuk, et al. 2012). He proposed a relationship between the synaptic input and synaptic output signal called as synaptic weight in the circuit given in Figure 2.14.

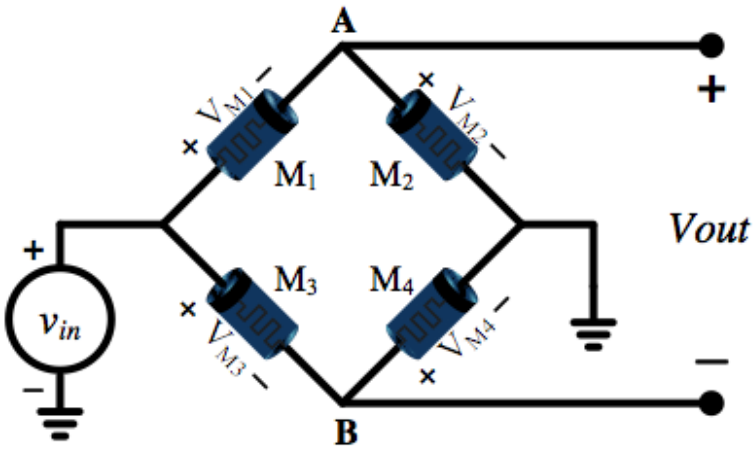

Figure 2.14: Memristor Wheatstone-bridge circuit(Chua, 2013)

The memristance of each memristor is charged by applying positive or negative pulses, $V_{in}(t)$. The memristance of M_1 and M_2 is decreased by positive pulses. The memristance of M_2 and M_3 is is increased by positive pulses.

The voltage V_A is greater than the voltage V_B with respect to the ground. It means that the circuit output voltage V_{out} is positive representing a positive synaptic weight. On the other hand, the output represents a negative synaptic weight when negative pulses are applied.

Memristor voltages are found via voltage-divider rule. The voltage V_{m1} is given as

$$V_{M1} = \frac{M_1}{M_1 + M_2} V_{in} \tag{2.34}$$

The voltage V_{M2} is given as

$$V_{M2} = \frac{M_2}{M_1 + M_2} V_{in} = V_A \tag{2.35}$$

The voltage V_{M3} is given as

$$V_{M3} = \frac{M_3}{M_3 + M_4} V_{in} \tag{2.36}$$

The voltage V_{M4} is given as

$$V_{M4} = \frac{M_4}{M_3 + M_4} V_{in} = V_B \tag{2.37}$$

The output voltage, equal to the voltage difference of nodes A and B, can be written as

$$V_{out} = V_A - V_B = \left(\frac{M_2}{M_1 + M_2} - \frac{M_4}{M_3 + M_4} \right) V_{in}$$

$$= \varphi . V_{in} \tag{2.38}$$

here φ is the synaptic weight given as

$$\varphi = \left(\frac{M_2}{M_1 + M_2} - \frac{M_4}{M_3 + M_4} \right). \tag{2.39}$$

Equation 2.39 represents the synaptic weighting operation. The input signal is weighted by Equation 2.39.

2.5 Logic Operations by Memristors

To be able to use memristors as a storage element, it is important to check their availability for basic logical operations. A cellular automaton model can be a useful model for these operations. It is a discrete model studied in computer science, mathematics, physics, complexity science, theoretical biology etc. It consists of a regular grid of cells. Each of these cells has a finite number of states (such as on and off or as in computer language system 0 and 1). An initial state (for t=0) is selected and every cell has the same rule for updating. It means that a new generation is formed according to the rule of the cellular automata. This rule is generally a mathematical function and it determines the new state of each cell. This determination depends on the current state of the cell and the states of the cells in the neighborhood.

A one-dimensional cellular automaton for the memristor logic operations has rows of cells and a set of rules (Chua-Itoh, 2009). The aim of the cellular automaton

forms the rules. As it has been mentioned, each cell can only be in two different states (on or off; 0 or 1; black or white etc.) and they have three neighbors, so there are 2^3=8 possible patterns for a neighborhood and there are 2^8=256 possible rules. Chua gives an example for a number 126 by using memristor cells with current pulse generator shown in Figure 2.15(Chua, 2013). It is known that the number 126 is written as '01111110' in binary representation. The rules are as follows:

1- 3 cells are white ⇒ the new state is white.

2- 3 cells are black ⇒ the new state is white.

3- Otherwise ⇒ the new state is black.

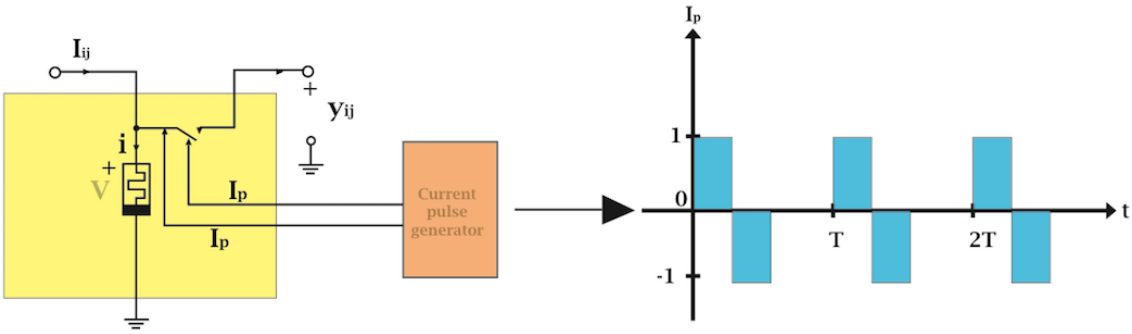

Figure 2.15: The memristor cell (a) with current pulse generator (b)

Each cell is coupled only to its left and right neighbor cell and '1' and '0' denote black and white, respectively. For instance, if three adjacent cells are as '101', it means that left cell is black, middle cell is white and right cell is again black. The next cell will become black according to the rule. Chua wrote the truth table for the number '126' as an example shown in Table 2.1.

Table 2.1:Truth table for the number 126

Current Pattern	111	110	101	100	011	010	001	000
New State for center cell	0	1	1	1	1	1	1	0

And its decimal representation is given in Table 2.2

Table 2.2: Decimal representation for the number 126

$(x_{i-1}(t), x_i(t), x_{i+1}(t))$	111	110	101	100	011	010	001	000
$w=2^2x_{i-1}(t) + 2^1x_i(t) + 2^0x_{i+1}(t)$	7	6	5	4	3	2	1	0
$x_i(t+1)$	0	1	1	1	1	1	1	0

where $x_i(t)$ denotes a state variable of the 'i'th cell. The left neighbor is (i-1)th neighbor of 'i'th cell and the right neighbor is (i+1)th neighbor of 'i'th cell. From Table 2.2, the relation can be summarized as

$$x_i(t+1) = \begin{cases} 0, & w = 0,7 \\ 1, & w = 1,2,3,4,5,6 \end{cases} \tag{2.40}$$

where $w \triangleq 2^2.x_{i-1}(t) + 2^1x_i(t) + 2^0x_{i+1}(t)$.

Chua used MxN rectangular array of memristor cells C(i,j) with Cartesian coordinate system. 'i' denotes the ith cell of 'M' and 'j' denotes the jth cell of 'N' and a current pulse generator produces I_p and it has positive and negative paired current pulses. If a positive current pulse is applied, the switch is turned on to be able to charge the memristor shown in Figure 2.16(Chua, 2013).

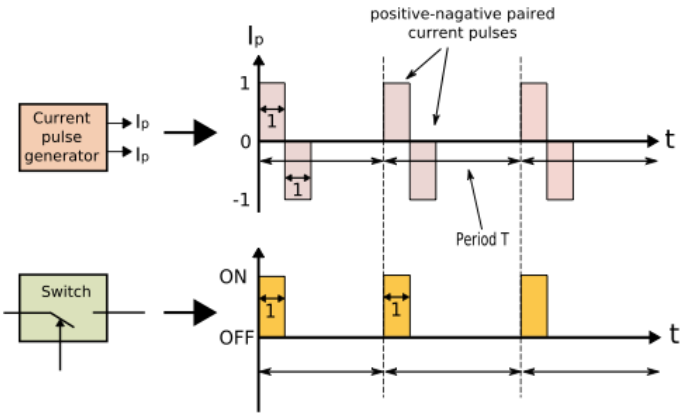

Figure 2.16: The positive and negative current pulses (a). The switch runs when the current pulse is positive (b).

As it has been mentioned, constitutive relation for the memristor is given as

$$V = M(q)i \tag{2.41}$$

and

$$i = W(\varphi)V \tag{2.42}$$

and the memristor characteristic relationship of flux-linkage and charge is given as

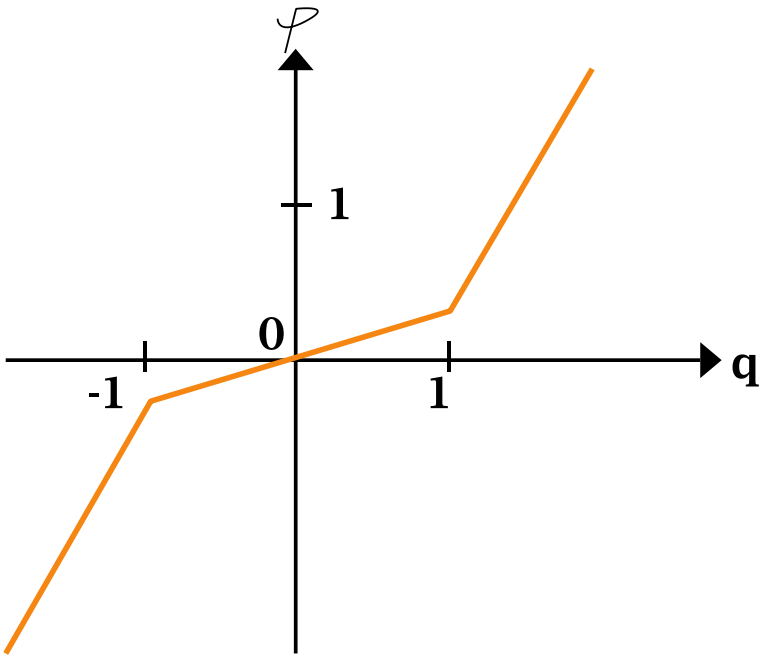

Figure 2.17: The memristor $q - \psi$ characteristic

The cell output $y_{ij}(t)$ is obtained as

$$y_{ij}(t) = \begin{cases} V(t) = M\big(q(t)\big).\, I_p(t), & I_p > 0 \\ 0, & I_p < 0 \end{cases} \tag{2.43}$$

with I_p=1.

The charge on the memristor is given as

$$q(t) = \int_0^t I_p(t)dt = \int_0^t 1dt = t \tag{2.44}$$

with I_p=1.

For 0≤t≤1 the current pulse I_p is equal to '1' then the voltage is obtained as

$$V(t) = M\big(q(t)\big)I_p(t) = M\big(q(t)\big) \tag{2.45}$$

It means that by applying a positive pulse, the memristance value of memristor is measured. This process is called as 'read process'. By using memristors, the basic logical operations can be emulated.

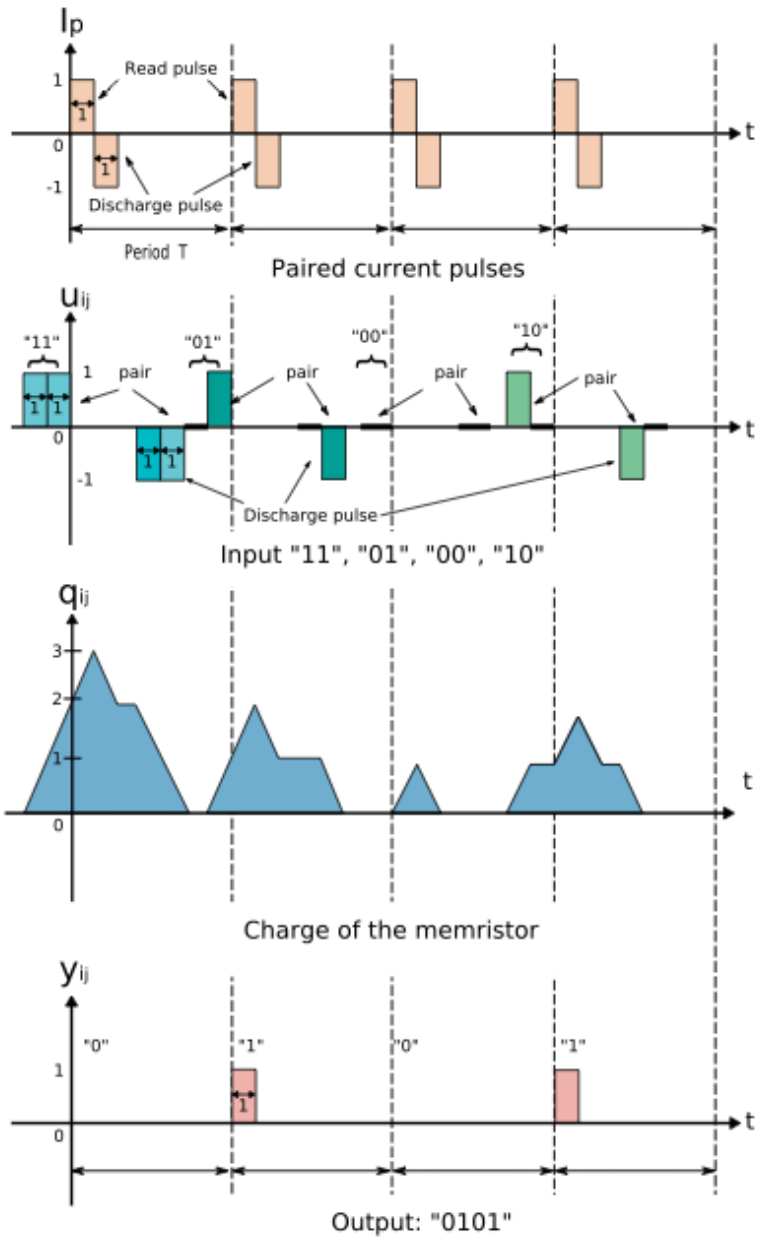

Figure 2.18. The positive and negative current pulses (a), and inputs for the logical operation ‘XOR’ (b). The obtained memristor charge (c) and the output (d) (Chua, 2009).

In Figure 2.18, a memristor cell with an input is shown for logical operations. The input current u_{ij} is applied to the cell as ‘11’, ’01’, ’00’, and ‘10’. The negative input pulses are applied to discharge the memristor. The read pulses are shown. It is important to notice that positive input pulses and negative input pulses are applied before and after the read pulse I_p, respectively. The obtained memristance is shown in Figure 2.19a(Chua, 2009).

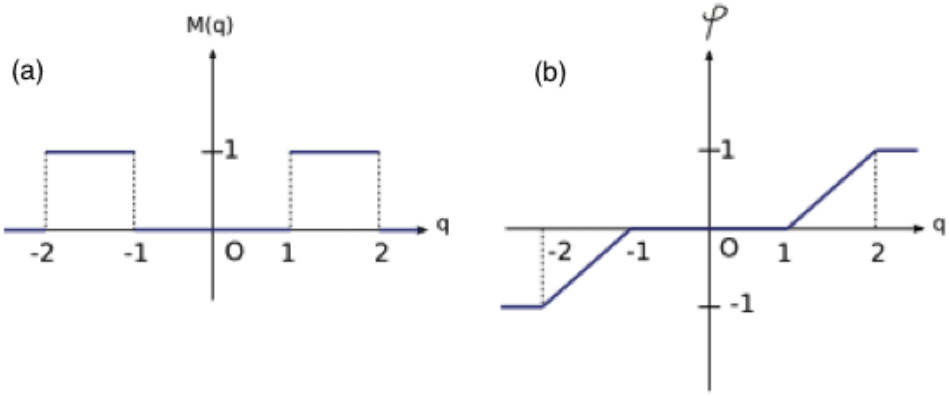

Figure 2.19: Memristance vs. charge (a), and the φ-q characteristic loci(b) for the logical operation 'XOR'

In Figure 2.20, the memristance M(q) is defined by

$$M(q) = \begin{cases} 1, & 1 \le q \le 2 \\ 0, & otherwise \end{cases} \tag{2.46}$$

and the output y_{ij} is defined by

$$y_{ij}(t) = V(t) = M\big(q(t)\big).I_p(t) \tag{2.47}$$

The cell output gives

$$y_{ij}(t) = \begin{cases} 1, & 1 \le q_{ij} \le 2 \\ 0, & otherwise \end{cases} \tag{2.48}$$

with $I_p>0$.

In Figure 2.18, it can be seen when the q_{ij} is between 1 and 2, the output y_{ij} gives '1', and otherwise it gives '0'. It is basically the logic operation for 'XOR'. The truth table for XOR is given in Table 2.3.

Table 2.3: The inputs and outputs for the logical operation ‘XOR’

u_{ij}		y_{ij}
0	0	0
0	1	1
1	0	1
1	1	0

If the input u_{ij} is given as in Table 2.4, the output will be as in Figure 2.21 with the memristance as shown in Figure 2.20.

Table 2.4: The inputs and outputs for the logical operation ‘AND’

u_{ij}		y_{ij}
0	0	0
0	1	0
1	0	0
1	1	1

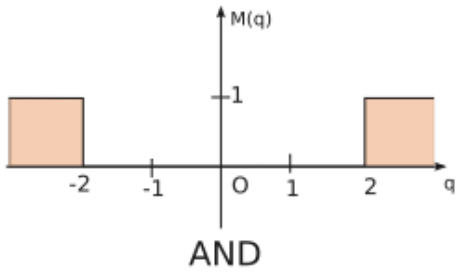

Figure 2.20: Memristance vs. charge loci for the logical operation ‘AND’.

The memristance M(q) shown in Figure 2.21 for the AND gate is given as

$$M(q) = \begin{cases} 1, & q \geq 2 \\ 0, & oth. \end{cases} \tag{2.49}$$

The output y_{ij} is shown in Figure 2.21 as

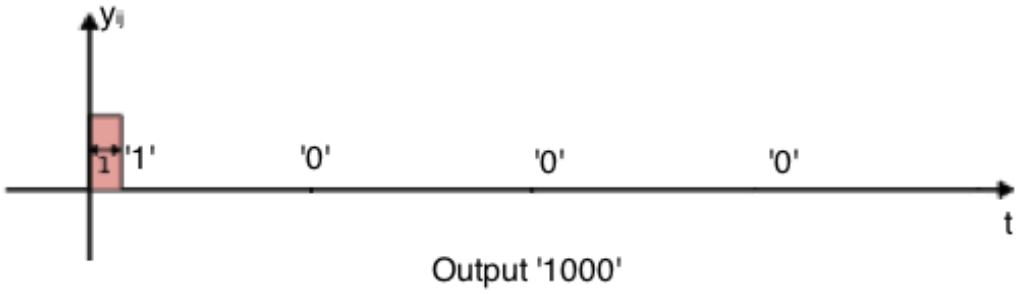

Figure 2.21: The output for the logical operation ‘AND’(Chua, 2009).

and it is summarized as

$$y_{ij} = \begin{cases} 1, & q \geq 2 \\ 0, & oth. \end{cases} \equiv \begin{cases} V(t) = M\big(q(t)\big).I_p(t), & q \geq 2 \\ 0, & oth. \end{cases} \tag{2.50}$$

It gives the logical operation of AND gate. For the other logical operations OR and XNOR, the truth tables are given as

Table 2.4: The truth table for the logical operation ‘OR’.

OR		
u_{ij}		y_{ij}
0	0	0
0	1	1
1	0	1
1	1	1

and

Table 2.5: The truth table for the logical operation ‘XNOR’.

XNOR		
u_{ij}		y_{ij}
0	0	1
0	1	0
1	0	0
1	1	1

They can be obtained by combining the memristance values. If the memristance is defined as

$$M_i(q) = \begin{cases} 1, & i \le q < i+1 \\ 0, & otherwise \end{cases} \tag{2.51}$$

it can be seen that the logical operation ‘AND’ can be obtained by $M_2(q)$; the logical operation ‘OR’ can be obtained by $M_1(q)+M_2(q)$; the logical operation ‘XOR’ can be obtained by $M_1(q)$; the logical operation ‘XNOR’ can be obtained by $M_0(q)+M_2(q)$. For the logical operation ‘OR’, the memristance value should be given in Figure 2.22(Chua, 2009).

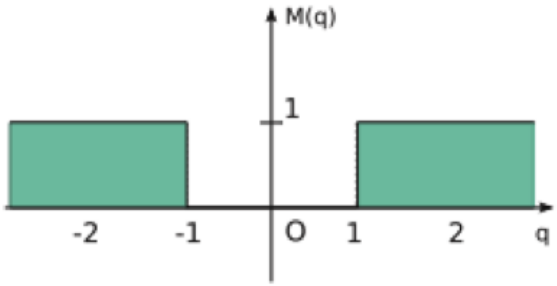

Figure 2.22: The memristance vs. charge loci for the logical operation ‘OR’(Chua, 09)

For the logical operation ‘OR’, $M_1(q)+M_2(q)$ gives

$$M_1(q) + M_2(q) = \begin{cases} 1, & 1 \le |q| < 3 \\ 0, & otherwise \end{cases} \quad (2.52)$$

For the logical operation 'XNOR', the memristance value should be given in Figure 2.23(Chua, 2009)

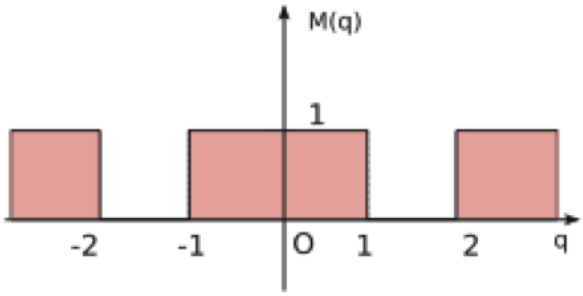

Figure 2.23: The memristance vs. charge loci for the logical operation 'XNOR'.

For the logical operation XNOR, $M_0(q)+M_2(q)$ gives

$$M_0(q) + M_2(q) = \begin{cases} 1, & |q| < 1 \; and \; 2 \le |q| < 3 \\ 0, & otherwise \end{cases} \quad (2.53)$$

CHAPTER 3

SYNAPTIC PLASTICITY

Modern neuroscience has deep feelings in biology, medicine, philosophy, physics, and mathematics(Mark F, 2001). The curiosity about how we see and hear, why we learn and forget, why we are angry or happy sometimes comes from the human nature. The study of the neuroscience is not old, but the study of the brain is of long standing. Scientists who work on the nervous system are distinctively from various scientific disciplines such as physics, medicine, biology, psychology, chemistry, and mathematics. Interdisciplinary work between these scientific disciplines is required to understand the nervous system. In general, the brain, spinal cord and nerves of the body are thought as the nervous system and they are crucial for life. With this system we are able to sense, move, and think.

Santiago R. Cahal (1852-1934) realized that neurons were discrete biological structures (Harth, et al. 1970). They sent and got information through their dendrites. His fascinating discovery was that there was a gap between the neurons and at that time nobody knew the nature of this gap (Jackson, 1995). Influenced by this invention, Charles S. Sherrington (1857- 1952) introduced a new concept, the synapse. A synapse can be described as a structure used by the neuron to send electrical and chemical signals to another neuron. The information is transferred from one neuron to another neuron via synapses. The term *synapse*, derived from a Greek word that means *to fasten*. The synapse has two sides called presynaptic and postsynaptic (Andy, 2013). The direction of information flow, which is from presynaptic to postsynaptic, determines the name of the synapse. Some molecular processes occur at the sides of the synapses to send information from the pre- to post-. In general, postsynaptic side is located on the axon terminal while the post side is on the soma or the dendrite shown in Figure 3.1.

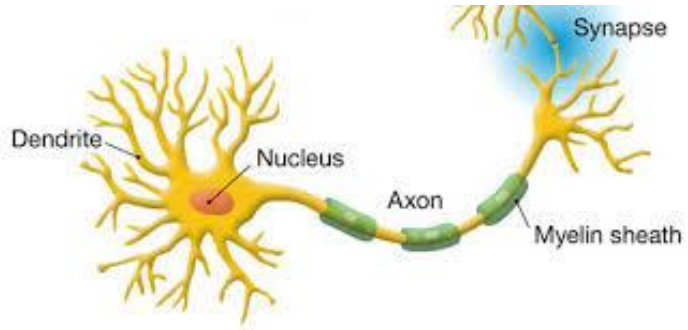

Figure 3.1 The neuron(Mark F, 2001)

The synapses are made up of two types, chemical synapse and electrical synapse (Mark, et al. 2001). In the chemical synapse, when the presynaptic neuron is stimulated, a chemical called neurotransmitter is released and then it is bound to the receptors on the postsynaptic cell. Chemical synapses are crucial for the biological computations that underlie thought. The electrical synapse has some special channels called gap junctions. These junctions pass the electric current directly. The distance between the electrical pre-synapse and post-synapse is about 3.5nm. Compared to chemical synapses, they conduct impulses faster. The signal in chemical synapse does not lack gain but in electrical synapse it does. The adult human brain contains 100-500 trillion synapses.

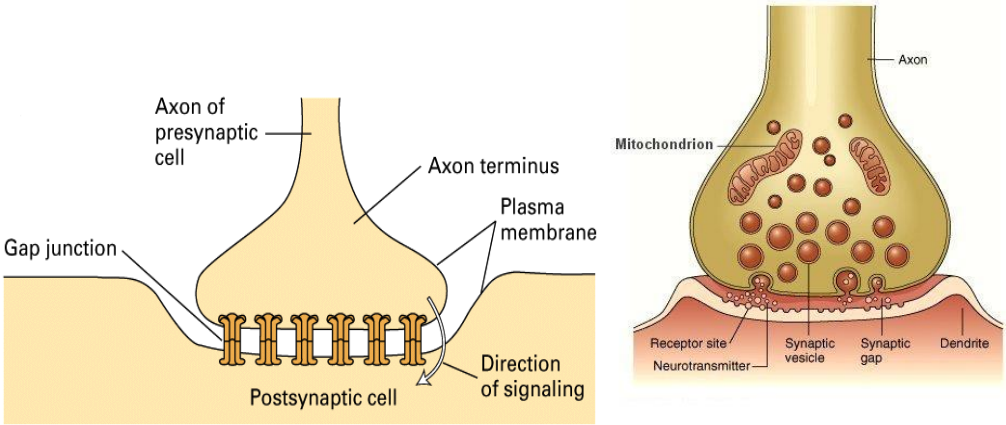

Figure 3.2 The electrical and chemical synapse(Mark F, 2001)

After a synapse is stimulated by an action potential, which will be given in detail later, the electrical stimulation is sent onto dendrites via synapses. These synapses are spread through the dendritic tree. Dendrites are important to determine which action potential is produced and why dendrites are covered by so many synapses. Some kinds of dendrites in cerebellum and cerebral cortex have spines. Spines that receive synaptic

inputs increase the receptive ability of the dendrite. This increased ability is thought to play a crucial role in learning, forgetting and memory functions of the brain. They are believed to have various chemical reactions that are activated by some types of synaptic activation.

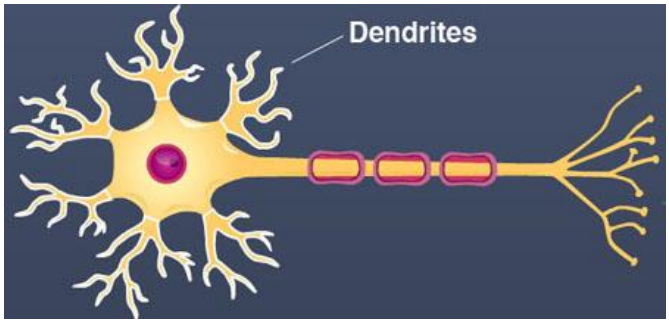

Figure 3.3 The dendrite

3.1 Neurons and Glia

Rudolf Carl Virchow, a German anatomist, recognized that the brain is filled up with neurons and glia cells. Glia, sometimes called neuroglia, provide support for neurons and nervous system (Kandel, 2007). One of the functions of glia is to hold the neurons in place. Some researchers nowadays consider glia to be the 'sleeping giants' (Nicola-Barres, 2009). They believed that one day it would be proven that glia contribute much more to information processing in the brain. Without glia, the brain cannot support its functions. Researchers currently know some functions of the glia cells. As it has been mentioned, they surround the neurons, keep them together and insulate the neuron from another. The glia cells are the oxygen suppliers of the neurons. They also wipe out the dead neurons. Neuroscientists have recently discovered that the glia cells play a crucial role on the physiological processes such as breathing (Alexander, 2010). They also help the neurons form new connections with the other neurons. They finally participate in the information transferring process and thereby play a crucial role in keeping the memory storage again.

Glia cells are separated into two categories based on their appearance in the microscope. The two types of glia cells are *astrocytes* and *oligodendrocytes*. Astrocytes regulate the chemicals in the glia by regulating the concentration of potassium ions in

the extracellular fluid (Mark, 2001). Researchers have recently discovered that these cell membranes have neurotransmitter receptors like neurons, and lead some events in the brain. The astrocytes activity is contributed to blood flow in the brain. The oligodendrocytes cells cover the axons in the central nervous system with their membrane. The electrical signals propagate more efficiently if the oligodendrocytes cells cover the axon.

Synapses, under communication, can strengthen or weaken over time. If they play a role for the communication, their abilities increase and if they do not, their abilities decrease. In neuroscience, this changeable ability for the activity of a neuron is called synaptic plasticity. The synaptic plasticity is one of the most important phenomena in brain because it is thought that it is responsible for the process of learning and memory (Mark, 2001). It can be formed by two rules for the synaptic plasticity. First, both pre-synaptic axon and post-synaptic neuron are active at the same time, and then the synapse is strengthened. Here the post-synaptic neuron is activated by other inputs. Hebb hypothesized for this situation that neurons that fire together wire together (Natalia-Dan, 2008). Second, the presynaptic axon is active, but the post-synaptic neuron is not strongly activated by other inputs, the synapse is then weakened. Hebb's hypothesized for this situation that neurons that fire out of sync lose their link (Hyun, et al. 2010). It can be seen that a neuron does not have any dominant effects on the firing rate of the post-synaptic neuron. It means that the correlation is essential for the synaptic plasticity. If a synapse is strengthened, there must be other stronger inputs that stimulate the post-synaptic neuron at the same time. Otherwise, the synaptic plasticity decreases if there are not any correlations between the inputs that stimulate the post-synaptic neuron.

The neurotransmitter, glutamate is the main transmitter that is responsible for the synaptic plasticity (Jackson, 1995). There are some receptors that are specialized for these neurotransmitters. They are the AMPA receptors and the NMDA receptors. They allow the positively charged ions to pass inside of the cell. AMPA and NMDA receptors are different from each other and they have also different tasks. The first difference between these receptors is that the conductance of NMDA receptor is based on Mg^{+2} ions. Mg^{+2} ions are the ions that clog the gate of NMDA receptor at the resting potential as shown in Figure 3.4.

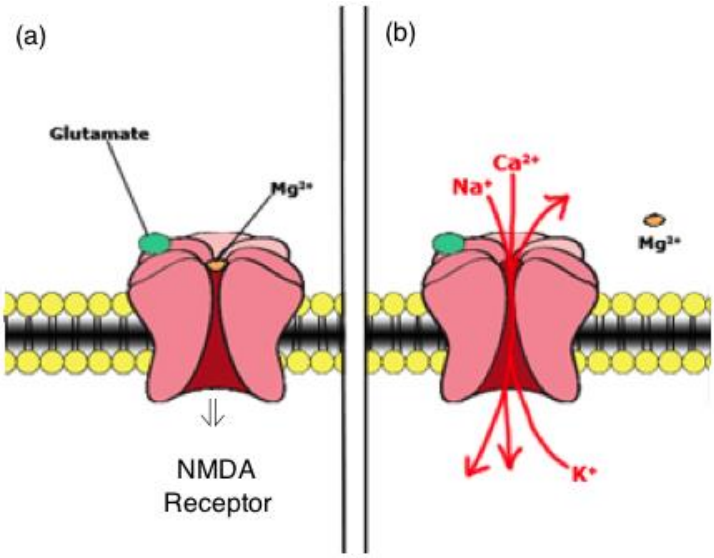

Figure 3.4 Glutamate binds to receptor (a), Mg^{+2} ion repels (b)

When an enough action potential arrives to the cell via AMPA receptors, the Na^{+} ions repel the Mg^{+2} ions from the NMDA receptor to the synaptic gap and this process is shown in Figure 3.4(Mark F, 2001). At this stage the NMDA gate is now open and it allows Ca^{+2} ions to pass through the gate and sodium ions K^{+} go out from the cell at the same time. Ca^{+2} ions can only pass through the NMDA receptor. This is the second difference between the NMDA receptor and AMPA receptor.

Ca^{+2} ions are important for the cell to activate some cellular reactions. If there is enough correlation between the inputs, Na^{+} ions that enter the cell via AMPA receptors repel Mg^{+2} ions and then Ca^{+2} enters the post-synaptic cell. Ca^{+2} ions trigger some mechanisms and make the synapse stronger. This process is called as 'long term potentiation'.

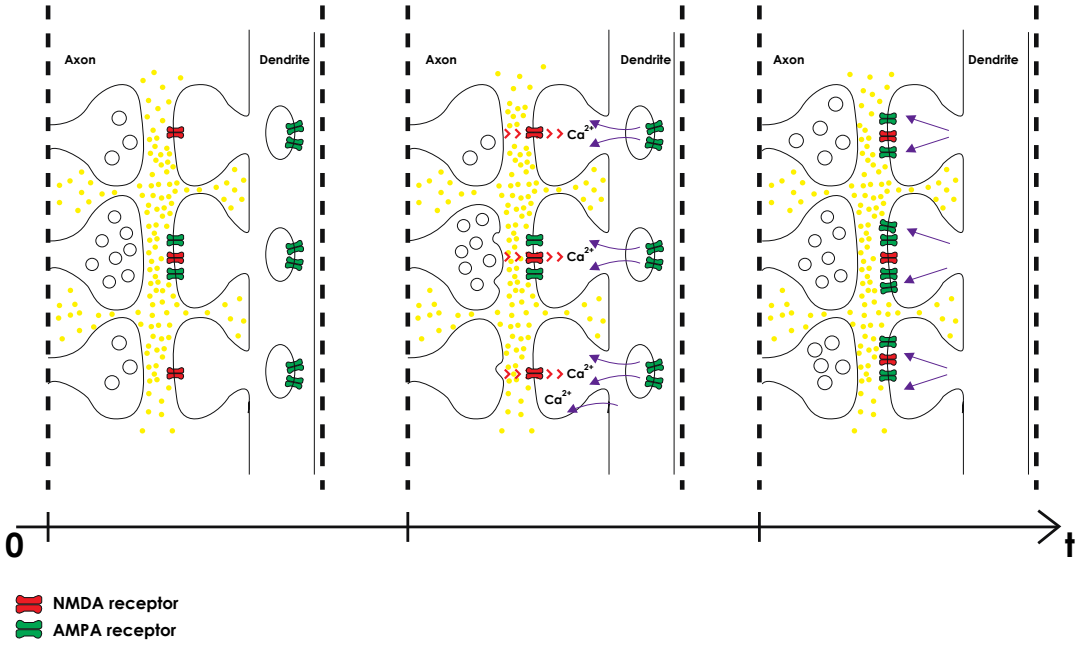

Figure 3.5 The process of occurrence of new AMPA receptors(Mark F, 2001)

If there is not enough correlation between the inputs, a few Ca^{+2} ions leak from NMDA receptor to the post-synaptic cell and they then trigger some different mechanisms and make the synapse weaker. This process is then called Long Term Depression (LTD).

3.2 The movement of Ions

Ion channels are made up of the membrane protein molecules (Izhikevich, 2007). The most important function of these channels is the selectivity properties. Most ion channels are specified by the diameter of their pole. The channel name depends on what kind of ions is permeable to that channel. If the channel is permeable to sodium ions, its name is Na^{+} channel. The calcium channels are permeable to Ca^{+2} ions and the potassium channels are permeable to K^{+} ions. These ions are also pumped by some enzymes, which are called ion pumps. These enzymes use the ATP energy that comes from mitochondria in glia to transport Na^{+} and Ca^{+2} ions from inside of the neuron to outside.

To move the ions through the channels, two processes, which are diffusion and electricity, are used in the cell. Diffusion also occurs in nature and it is a transport

phenomena. Therefore, there will be a net ion flow from the high concentration region to low concentration region. This movement is called ‘diffusion’. Due to the fact that ions are electrically charged particles, an electromagnetic field should occur. This electromagnetic field can trigger the movement of the ions in the cell.

In a biological cell, the membrane potential is the difference in potential between the interior and exterior in that cell, which is shown in Figure 3.6. The outside of the neuron is electrically positive with respect to the inside. This difference is called membrane resting potential. Without any excitation, this resting potential is maintained. The membrane potential can be measured by the ionic concentrations on either side of the membrane.

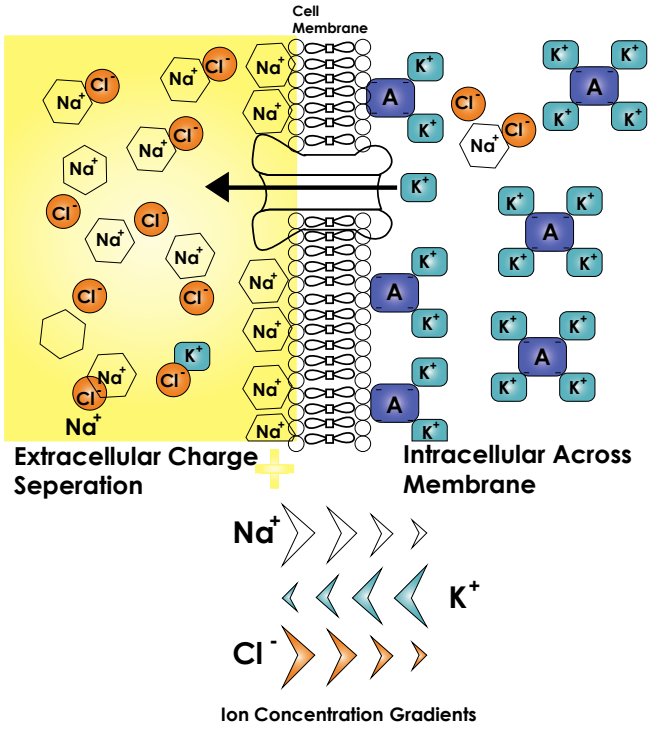

Figure 3.6 Extracellular and intracellular ion concentrations

For the membrane in Figure 3.6, the inside concentration of the membrane has more potassium ions, K^+, the outside concentration of the membrane has more Na^+ and Ca^{+2} ions(Mark F, 2001). As it has been mentioned before two ionic pumps are important in the membrane. They are Sodium-Potassium Pump and Calcium Pump. After the breaking down of ATP, this released energy is used by the pumping systems. The pump exchanges the Na^+ with K^+. This pumping process requires energy because the pump pushes ions against the concentration gradients. It is thought that the sodium-

potassium pump requires at least 70% of the energy of ATP in the brain. The calcium pump is also an enzyme that pushes Ca^{+2} to outside of the cytosol. There are some additional pumping mechanisms to decrease the Ca^{+2} level such as calcium binding proteins and some organelles. In 1952 Hodgkin and Huxley derived a model that explains how action potentials propagated in the squid giant neurons (Hodgkin-Huxley, 1952). The model was based on the ionic currents.

Information is transferred via ionic currents through neuron membranes. These membrane currents are sodium (Na^+), potassium (K^+), calcium (Ca^{+2}), and chloride (Cl^-). Concentrations of these ions are different on the inside and the outside of a cell. This difference between the inside and the outside is called electrochemical gradients. The outside of the neuron has a high concentration of Na^+ and Cl^-. The cell membrane decides which ions can flow through the channels.

3.2.1 The Nerst Potential

K^+ ions are sent out from inside of the cell because inside of the cell K^+ concentration is higher than the outside K^+ concentration. Since K^+ ions carry a positive charge and thereby, they produce the outward current. This ion transfer creates an electric potential gradient across the membrane called membrane voltage (Strukov, et al. 2009). Then it ends because K^+ ions are attracted to the negatively charged interior. At the same time they are also repelled from the positively charged exterior of the membrane. When the inside ion concentration of the cell and outside ion concentration of the cell are equal, this potential is called equilibrium potential. This potential depends on the ion concentrations and the value of this potential is given by the Nerst equation. The Nerst equation is given by

$$E_{ion} = \frac{RT}{zF} \ln\left(\frac{[Ion]_{out}}{[Ion]_{in}}\right) \tag{3.1}$$

'$[Ion]_{in}$' is the inside concentration of the ions. '$[Ion]_{out}$' is the outside concentration of the ions. 'R' is the universal gas constant and 'T' is the temperature in Kelvin. 'F' is the Faraday's constant. 'z' is the valance of the ions (z=1 for Na^+ and K^+; z=-1 for Cl^- ; z=2 for Ca^{+2}).

For the neuron of a mammalian, the Nerst equilibrium potential is calculated as

$$E_{ion} \cong 62log\frac{[Ion]_{out}}{[Ion]_{in}}\ mV \tag{3.2}$$

Thus for Na^+, K^+, Cl^- and Ca^{+2} ions, the Nerst equilibrium potentials are 90mV, -90mV, -89mV, and 146mV, respectively.

3.2.2 Ionic Currents and Conductances:

Hodgkin and Huxley model is a mathematical model that describes how action potentials in neurons are initiated. They described the model in 1952 to explain the ionic mechanism underlying the initiation of action potentials in the squid giant axon and received the Nobel Prize in Physiology or Medicine in 1963. They defined an equivalent circuit that defines the gate currents as given in Figure 3.7(Izhikevich, 2007).

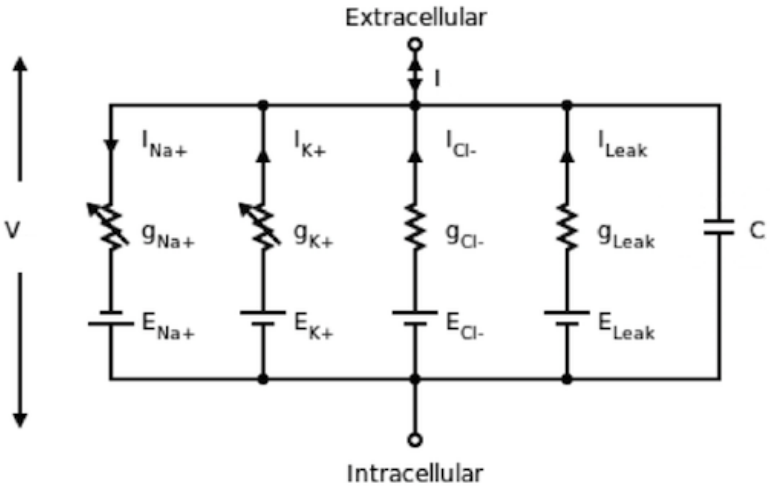

Figure 3.7 Hodgkin-Huxley Model Circuit(Izhikevich, 2007)

If the membrane potential V is equal to the equilibrium potential, the net K^+ current is zero and the current is defined by

$$I_K = g_K(V - E_k) \tag{3.3}$$

where g_K (mS/cm^2) is the K^+ conductance and (V - E_K) is the force that drives K^+ ions. For the other ions, the currents can be described by

$$I_{Na} = g_{Na}(V - E_{Na}) \tag{3.4}$$

$$I_{Ca} = g_{Ca}(V - E_{Ca}) \tag{3.5}$$

$$I_{Cl} = g_{Cl}(V - E_{cl}) \tag{3.6}$$

In neurons, conductance is time-dependent. The total current, I, is equal to the membrane capacitive current, $C\dot{V}$, plus all the other ionic currents. From the equivalent circuit the total current is given by

$$I = C\dot{V} + I_{Na} + I_{Ca} + I_K + I_{Cl} \tag{3.7}$$

with Equations (3.6), (3.7), (3.8), (3.9) it is

$$C\dot{V} = I - g_{Na}(V - E_{Na}) - g_{Ca}(V - E_{ca}) - g_K(V - E_K) - g_{Cl}(V - E_{Cl}) \tag{3.8}$$

If there is no ion passes from exterior to interior or interior to exterior, this condition is called as resting potential of the membrane.

3.2.3 Resting Potential and Input Resistance:

Ions can flow through the ionic channels. Gates on the membrane control the electrical conductance of the channels. Three factors affect these gates: Membrane potentials (Na^+ or K^+ channels), intracellular agents and extracellular agents (neurotransmitters, AMPA and NMDA receptors). The net current generated by a large population is described by

$$I = \bar{g}p(V - E) \tag{3.9}$$

'$\bar{g}$' is the maximal conductance of the population and 'E' is the reverse potential of the current and 'p' is the proportion of the open channels.

3.2.4 Voltage-gated Channels:

If gates are sensitive to the membrane potential, the channels are said to be voltage-gated. Hodgkin and Huxley described the probability of an activation gate by the variable 'm' (sometimes n is used for K^+ and Cl^- channels). They also described the probability of an inactivation gate by the variable 'h'. For the large population, the proportion of open channels is given by

$$p = m^a h^b \tag{3.10}$$

where 'a' is the number of activation gates and 'b' is the number of inactivation gates. For the activation parameter 'm', if its value is between zero and one, the channel is said to be partially active. If 'm' is equal to one, the channel is completely activated. If 'm' is equal to zero, the channel is deactivated. The dynamics of the activation variable 'm' is described by

$$\frac{dm}{dt} = \frac{m_\infty(V) - m}{\tau(V)} \tag{3.11}$$

where $m_\infty(V)$ is the steady state activation function and $\tau(V)$ is the time constant. They were measured experimentally. The dynamics of the inactivation variable 'h' is described by

$$\frac{dh}{dt} = \frac{h_\infty(V) - h}{\tau(V)} \tag{3.12}$$

where $h_\infty(V)$ is the steady-state inactivation function and $\tau(V)$ is the time constant. They were measured experimentally.

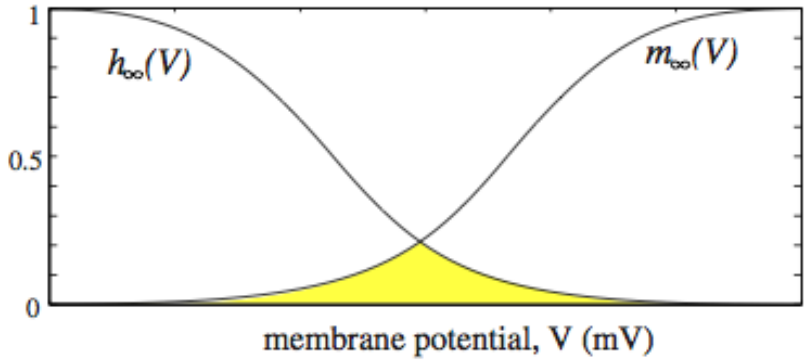

Figure 3.8 Activation (m) and inactivation function (h) (Izhikevich, 2007)

3.3 Hodgkin-Huxley Equations:

Hodgkin and Huxley determined that squid giant axon carriers have three major-currents. Currents are:

1- Voltage-gated K^+ currents with four activation gates, n^4
2- Voltage-gated Na^+ currents with three activation and one inactivation gate, m^3h
3- Leak currents, I_L

The Equation 3.7 with these gates is given as

$$C\dot{V} = I - \bar{g}_K n^4 (V - E_K) - \bar{g}_{Na} m^3 h (V - E_{Na}) - g_L (V - E_L) \tag{3.13}$$

where

$$\frac{dn}{dt} = \alpha_n(V)(1 - n) - \beta_n(V)n \tag{3.14}$$

$$\frac{dm}{dt} = \alpha_m(V)(1 - m) - \beta_m(V)m \tag{3.15}$$

$$\frac{dh}{dt} = \alpha_h(V)(1 - h) - \beta_h(V)h \tag{3.16}$$

The standard notations of these functions are given as

$$\frac{dn}{dt} = \frac{n_\infty(V) - n}{\tau_n(V)} \tag{3.17}$$

$$\frac{dm}{dt} = \frac{m_\infty(V) - m}{\tau_m(V)} \tag{3.18}$$

$$\frac{dh}{dt} = \frac{h_\infty(V) - h}{\tau_h(V)} \tag{3.19}$$

where $n_\infty = {\alpha_n}/{\alpha_n + \beta_n}$, $m_\infty = {\alpha_m}/{\alpha_m + \beta_m}$ and $h_\infty = {\alpha_h}/{\alpha_h + \beta_h}$ with $\tau_n = 1/(\alpha_n + \beta_n)$, $\tau_m = 1/(\alpha_m + \beta_m)$ and $\tau_h = 1/(\alpha_h + \beta_h)$.

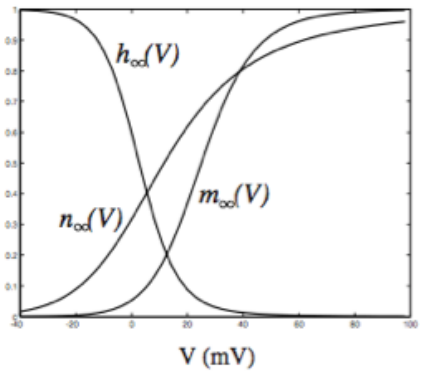

Figure 3.9 Activation and inactivation functions and time constants(Izhikevich, 07)

The functions $\alpha(V)$ and $\beta(V)$ describe the transition rates between open and close states of the channels. Hodgkin and Huxley described them as

$$\alpha_n(V) = \frac{0.01(V - 10)}{\exp\left(\frac{V - 10}{10}\right) - 1} \tag{3.20}$$

$$\alpha_m(V) = \frac{0.1(V-25)}{\exp\left(\frac{V-25}{10}\right)-1} \tag{3.21}$$

$$\alpha_h(V) = 0.7\exp(\frac{V}{20}) \tag{3.22}$$

$$\beta_n(V) = 0.125\exp(\frac{V}{80}) \tag{3.23}$$

$$\beta_m(V) = 4\exp(\frac{V}{18}) \tag{3.24}$$

$$\beta_h(V) = \frac{1}{\exp\left(\frac{V-30}{10}\right)+1} \tag{3.25}$$

3.4 Action Potential:

The membrane potential quickly rises and falls and this short-lasting event is called ‘Action Potential’. In Figure 3.10 an action potential of the Hodgkin-Huxley model stages are given.

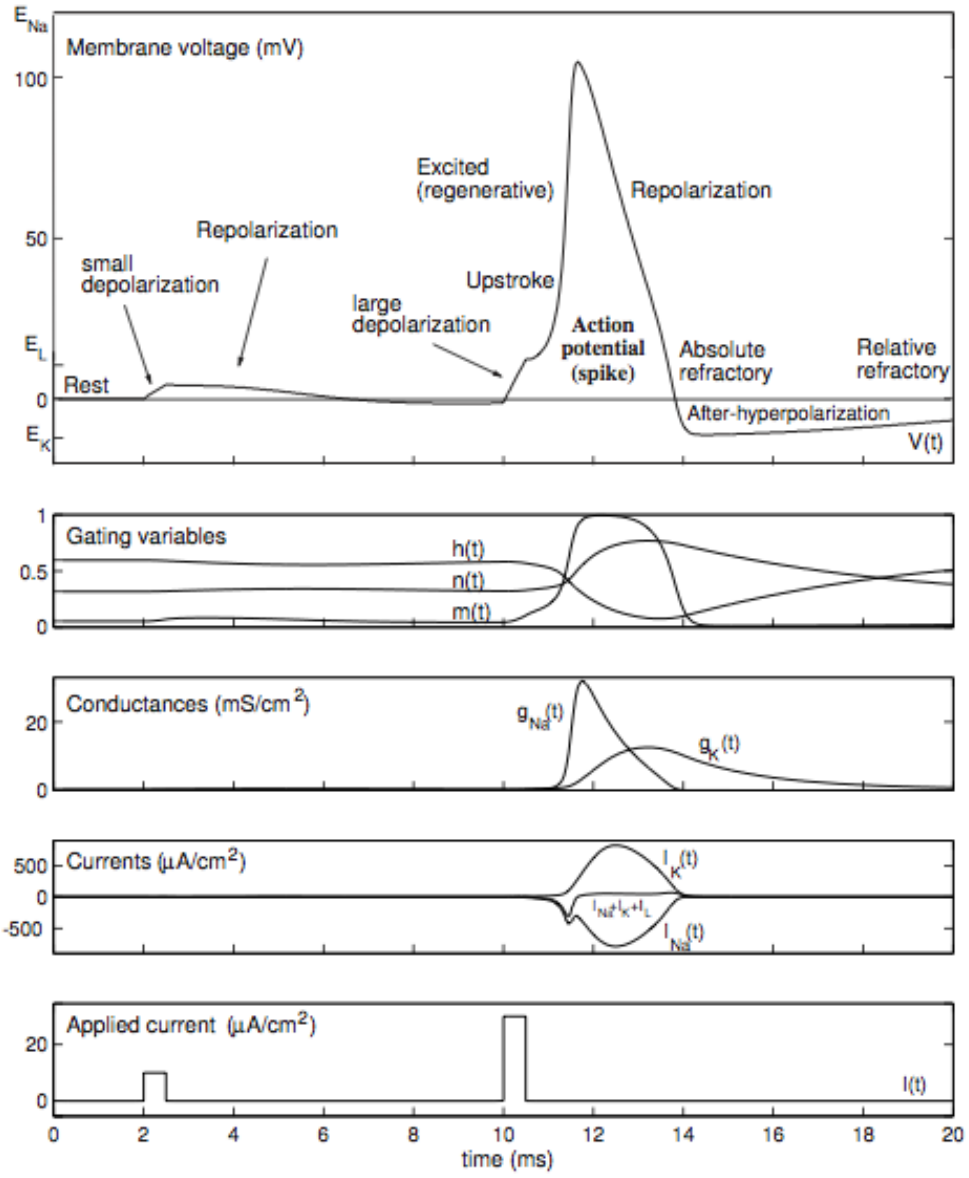

Figure 3.10 A phase to phase incoming action potential(Izhikevich, 2007)

If a small pulse of current is applied, it produces a small perturbation of the membrane potential called as depolarization. Then the membrane voltage returns to its resting potential. This process is called repolarization and it is shown in Figure 3.10. For t=10ms, a big pulse of current is applied to the membrane and it causes a strong depolarization. It is called as 'action potential' or 'spike'.

The variables 'm' and 'n' are increased by the strong depolarization approximately at 12ms. Since g_{Na} is big and the time constant is small, variable 'm' is fast. While 'h' goes to zero, the Na^+ current is inactivated and while 'n' goes to one the current K^+ is slowly activated. At the process of after-hyperpolarization, V is near V_{rest}.

The Hodgkin-Huxley system cannot generate another spike while Na^+ current continues to be inactivated. This period is called absolute refractory period. At the period of relative refractory period, the system is available to produce a new spike.

To describe the propagation of the action potential, a potential V(x,t) should be added because V(t) does not depend on the time. The new equation is formed as

$$CV_t = \frac{a}{2R}V_{xx} + I - I_K - I_{Na} - I_L \tag{3.26}$$

This equation is called as the Hodgkin-Huxley cable equation.

In 2012 Chua, et al. used memristors in the Hodgkin-Huxley model of squid giant axon (Chua, et al. 2012). They noticed that time varying resistors obey the memristor characteristics and they replaced them with memristors. It is important to remember the characteristics of memristor which is the instantaneous terminal current i(t) and V(t) obey Ohm's law. It is given as Equation 3.27

$$V = Ri \tag{3.27}$$

$$R = R(x_1, x_2, \dots, x_n) \tag{3.28}$$

where $\mathbf{x} = (x_1, x_2, \dots, x_n)$ is the state variables. The memristor state equation as a function of current is given as

$$\boldsymbol{x} = \boldsymbol{f}(\boldsymbol{x}, i) \tag{3.29}$$

The state variables are independent of any electrical variables. They might be temperature, pressure etc. The number of 'n' is the order of the complexity of the memristor dynamics.

The memristor state equations as a function of voltage can be also described as

$$\boldsymbol{x} = \boldsymbol{f}(\boldsymbol{x}, V) \tag{3.30}$$

where the Equation 3.30 is considered as

$$i = GV \tag{3.31}$$

$$G = G(x_1, x_2, \dots, x_n) \tag{3.32}$$

The continuous function G=G(**x**) is called memductance (Siemens).

They realized that R_K obeys the characteristics of the first order memristor.

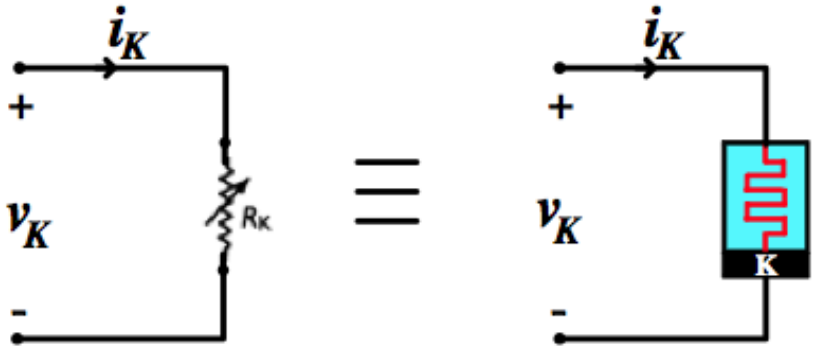

Figure 3.11 Time varying resistance replaced by a memristor(Chua, 2011)

Then they rewrote the potassium current equation, $I_K = \bar{g}_K n^4 (V - V_K)$ as

$$i_K = G_K(x_1) V_K \tag{3.33}$$

and

$$G_K(x_1) = \bar{g}_K x_1^4 \tag{3.34}$$

They changed the symbol as follows

$$n \rightarrow x_1$$

Then Hodgkin-Huxley equations can be written as

$$\frac{dx_1}{dt} = \alpha_n(1 - x_1) - \beta_n x_1 \tag{3.35}$$

$$= \left\{ \frac{0.01[(V_K + E_K) + 10]}{\exp\left[\frac{(V_K + E_K) + 10}{10}\right] - 1} \right\} (1 - x_1) - 0.125 \left\{ \exp\left[\frac{(V_K + E_K)}{80}\right] \right\} x_1$$

$$\triangleq f_n(x_1, V_K) \tag{3.36}$$

where E_K=12mV. If the voltage V_K is applied as

$$V_K = 0.05\sin(100t) \tag{3.37}$$

the loci of i_K and V_K gives the pinched-hysteresis loop as shown in Figure 3.12.

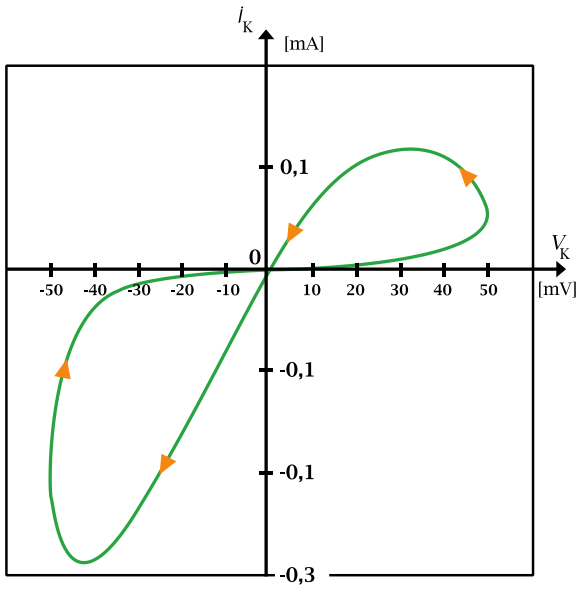

Figure 3.12 The pinched hysteresis loop of potassium ion channel memristor(Chua, 13)

They also realized that R_{Na} obeys the characteristics of the second order memristor. Second means that there are two different variables such as ‘n’ and ‘h’.

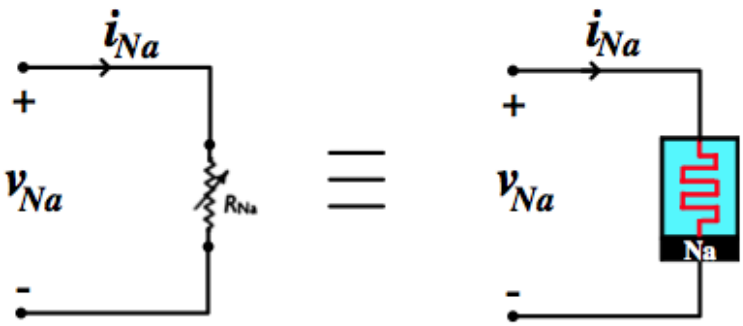

Figure 3.13 Time varying resistance replaced by a memristor(Chua, 2013)

Then they rewrote the sodium current equation, $\bar{g}_{Na}m^3h(V-E_{Na})$ as

$$i_{Na} = \bar{g}_{Na}x_1^3x_2V_{Na} \tag{3.38}$$

They changed the symbols as follows

$$V_{R_{Na}} \rightarrow V_{Na}$$

$$m \rightarrow x_1$$

$$h \rightarrow x_2$$

With these changes the Hodgkin-Huxley equations can now be written as

$$\frac{dx_1}{dt} = \left\{\frac{0.1[(V_{Na}-E_{Na})+25]}{\exp\left[\frac{(V_{Na}-E_{Na})+25}{10}\right]-1}\right\}(1-x_1) - 4\left\{\exp\left[\frac{V_{Na}-E_{Na}}{18}\right]\right\}x_1$$

$$= f_m(x_1, V_{Na}) \tag{3.39}$$

$$\frac{dx_2}{dt} = \left\{0.07\exp\left[\frac{(V_{Na}-E_{Na})}{20}\right]\right\}(1-x_2) - \left\{\frac{1}{\exp\left[\frac{(V_{Na}-E_{Na})+30}{10}\right]+1}\right\}x_2$$

$$= f_h(x_2, V_{Na}) \tag{3.40}$$

where E_{Na} =115mV. If the voltage V_{Na} is applied as

$$V_K = 0.05\sin(1500t) \tag{3.41}$$

the loci of i_{Na} and V_{Na} gives the pinched-hysteresis loop as shown in Figure 3.13.

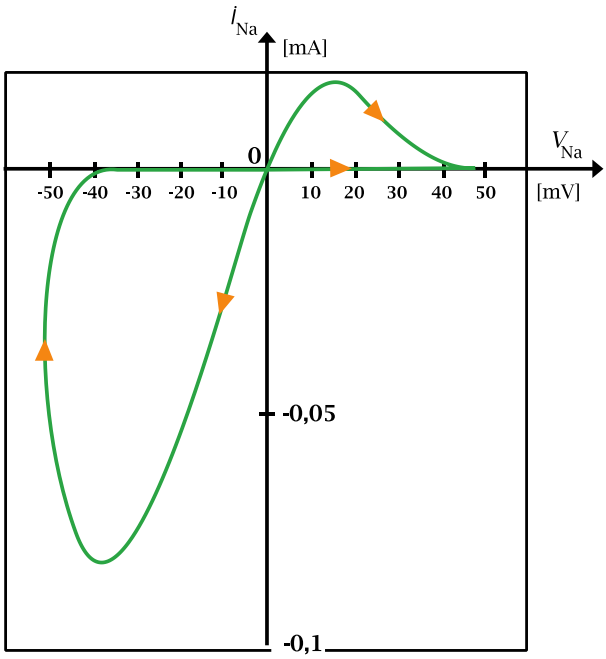

Figure 3.14 The pinched hysteresis loop of potassium ion channel memristor(Chua, 13)

These hysteresis loops indicate that time-variant resistances in the Hodgkin-Huxley model obey the memristor characteristics, so it was understood that they were actually memristors.

3.5 The Process of Long-Term Potentiation

When enough glutamates are released and enough Na^{+} ions enter the post-synaptic neuron through AMPA receptor, Mg^{+2} ions that clog the NMDA receptor are repelled by these Na^{+} ions. It is the signal for the Ca^{+2} ions to enter the post-synaptic cell through the NMDA receptor. Ca^{+2} ions trigger some reactions and as a result of these reactions, new AMPA receptors settle on the synapse of the post-synaptic neuron. The new AMPA receptor makes the synapse stronger.

An experiment for the effectiveness of the Schaffer collateral synapses on the neurons of hippocampus is recorded. This experiment is done by giving electrical stimulus to that part (Dale, 2008). This electrical tetanus is the high frequency tetanus such as 50 to 100 stimuli at frequency of 100. This kind of tetanus causes long-term potentiation (LTP) and the effectiveness of postsynaptic potentiation (EPSP) is

strengthened. The important feature of the hippocampal region of the brain is that it is input-specific shown in Figure 3.15. Some inputs may not cause LTP. It means that every high-frequency input cannot cause LTP. Another important feature of the LTP is that the input for LTP lasts approximately a few seconds, but LTP might last weeks, months or even a lifetime. As it has been mentioned, not only high frequency is required to induce LTP but also the correlation between the inputs are required to induce LTP. It means that it is required that enough inputs must activate to the synapse to induce LTP.

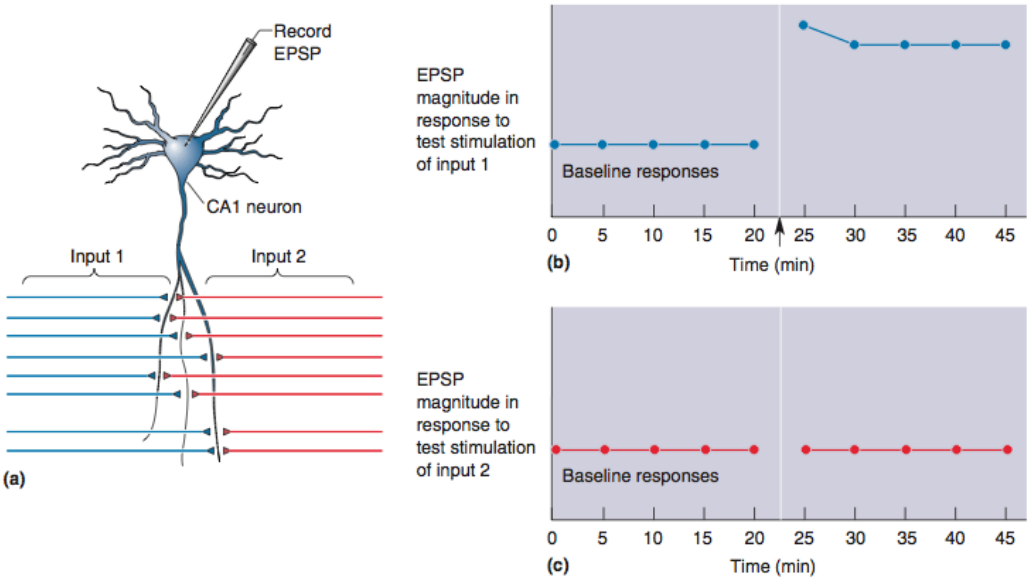

Figure 3.15 EPSP results of different inputs for LTP(Mark F, 2001)

When glutamates are released, Na^{+} ions enter the cell through the AMPA receptors. When they are enough to repel the Mg^{+2} ion-blocking on the NMDA receptor, Ca^{+2} ions enter the cell through the NMDA receptor gate. This amount of Ca^{+2} ions is the signal to activate two protein kinases. The first one is Protein Kinase C, and the second one is Calcium-Calmodulin-Dependent Protein Kinase II, CAMKII. These protein kinases activate the cellular mechanisms that cause to relocate the new AMPA receptors to the synaptic gap of the post-synaptic neuron and cause LTP as shown in Figure 3.16.

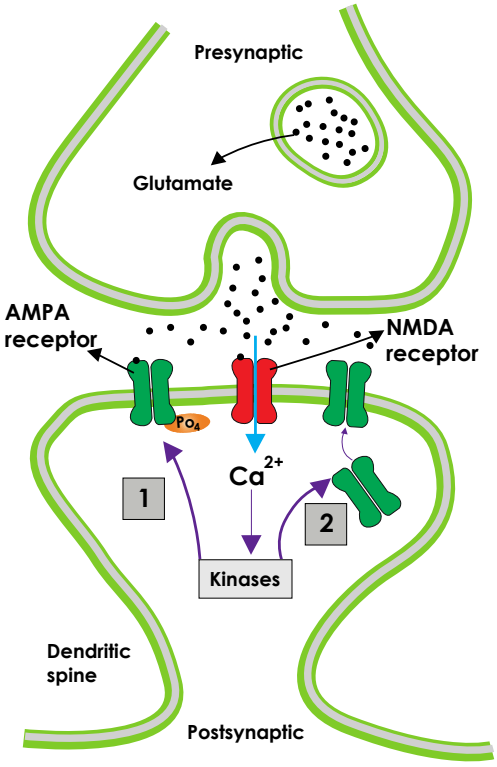

Figure 3.16 The chemical reactions for new AMPA receptors(Mark F, 2001)

3.6 The Process of Long-Term Depression

Neurons that fire out of sync lose their link. If the uncorrelated input arrives to dendrites of the post-synaptic cell, the synapse is weakened. Depression can be created by influxing less Ca^{+2} ions to the post-synaptic cell (Ruth, et al. 2009). These amounts of Ca^{+2} ions trigger some reactions and as a result of these reactions, the AMPA receptor is withdrawn. The synaptic plasticity is now weakened and this process is called the long-term depression.

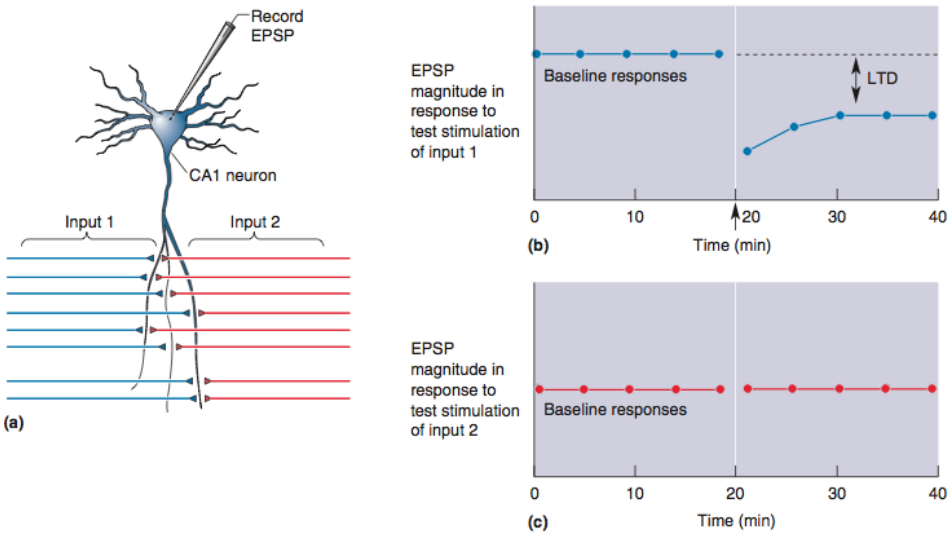

Figure 3.17 EPSP results of different inputs for LTD(Mark F, 2001)

When the post-synaptic cell is weakly activated by its inputs, it means that less Ca^{+2} ions enter the post-synaptic cell through the NMDA receptor, then the post-synaptic cell undergoes to LTD. The other experiment is made by giving low-frequency tetanus (1 to 5 Hz.) to the Schaffer collateral synapses on the CA1 neurons of the hippocampus. After this tetanus, Mg^{+2} ion-blocking is protected on NMDA receptor, but some Ca^{+2} ions escape to the cell through this receptor and make the neuron weakly depolarized. On the contrary of LTP, this amount of Ca^{+2} ions trigger the protein phosphatases enzymes. As a result of these enzymes, AMPA receptors are withdrawn from the synapse.

Ca^{+2} ions are the most important signals to the synapses for both the LTP and LTD. Different levels of Ca^{+2} ions can cause LTP or LTD as shown in Figure 3.18. For the hippocampus, if the calcium ion level is more than 5μM, the protein kinase is activated and new AMPA receptors are relocated to the synaptic gap. This process causes LTP. If the calcium ions level is less than 1μM, the protein phosphatase enzymes are activated and AMPA receptors are withdrawn. This process makes the synapse weaker and it causes LTD. All these processes use ATP energy via mitochondria. The energy for these mechanisms is supported by glia part of the brain.

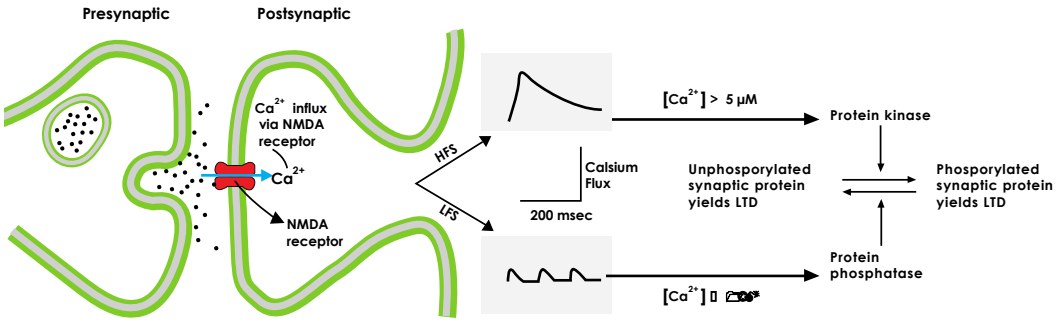

Figure 3.18 Different influx of Ca^{+2} ions causes LTP or LTD(Barry, 2001)

Some NMDA receptor blocking chemicals were put into the brains of rats for an experiment, and then their ability to escape from mazes was observed (Mark, 2001). On the contrary of normal ones, they are not able to learn the ways to escape from mazes. Scientists with these kinds of experiments believed that NMDA receptors play a crucial role on learning and memory processes.

3.7 Simple Learning Systems

The invertebrate creatures have been frequently used for different experiments. The squid is one of the best known of them with its contribution of giant axon and giant synapse to understanding of cellular neurophysiology. Additionally, flies, cockroaches, bees, leeches and worms are used for different purposes in the experiments. The advantages of using invertebrate creatures for neuroscience experiments can be listed as follows:

- The total number of the neurons of the nervous system is small: The invertebrate creatures have less neurons than a human brain.

- The size of the neurons is large: Some of the invertebrate creatures have very large neurons, which enables a scientist to study easily on electro-physiologically.
- Easy categorization is possible: Invertebrates have neurons that can be classified by considering size, location and electrophysiological properties and can be categorized separately.
- Identifiable circuits: Same connections between neurons can be organized separately by identifiable neurons.
- Basic genetics: The structure of the nervous system of the invertebrates includes small genomes and rapid cycles that make them an easy sample to study for genetic and molecular biological basis of learning.

The invertebrates are extremely important in understanding of the neural behavior. It is true that the existing collected data about the behavior is in a limited amount. Nevertheless, it is observed that many of the invertebrate species are performing the same simple forms of learning such as habituation, sensitization, and classical conditioning. The sea slug named *Aplysia Californica* has been used to examine the neurobiology of learning (Chua, 2013).

3.7.1 Nonassociative Learning in Aplysia

You definitely blink when someone blows gently at your eye. In the end, assuming that the air puffs are not harmful, you will habituate. Correspondingly a spray of water is spurted over a fleshy region of Aplysia called as the siphon, the gill will pull back. This is named as gill-withdrawal reflex. It is the same reflex displayed as the eye blink, that is habituation after repeated presentation of the water jet. Eric Kandel and his colleagues at Colombia University have begun doing experiments in 1960s about determining where the procedural memory resides and how it is formed. These pioneering experiments were recognized with the Nobel Prize at Medicine in 2004.

3.7.2 Habituation of the Gill-Withdrawal Reflex

The sensory data from the siphon is carried along a nerve until it enters a region of the Aplysia nervous system called the abdominal ganglion. In that part, the information is distributed to motor neurons and to interneurons. One of the motor neurons, which are receiving the direct monosynaptic sensory input from the siphon, is named as L7, and it is the cell that is innervating the muscles, which are making the gill-withdrawal reflex. For that reason, the research focuses on how this monosynaptic cycle changes during habituation (Mark, 2011).

The initial question deals with where the habituation occurs. When the siphon skin is repeated, the gill-withdrawal muscles react progressively less than the previous ones. This difference that makes the habituation remarkable might be because of several reasons. Firstly by squirting the water, the act of it decreases at the sensory nerve endings. Second the motor neuron makes it less responsive to the synaptic stimulation at muscles and the third place is the synapse between the motor neuron and the sensory neuron.

They made some microelectrode recordings from the sensory neuron when the habituation occurred. The fire action potentials are transferred by the sensory neuron as a response to skin stimulation. At the same time, motor response decreased. Correspondingly, the third possibility is dismissed by electrically stimulating the motor neuron as it always brings the same amount of muscle contraction. In the end, the second possibility reveals that the habituation occurs at the synapse joining the sensory input to the motor neuron. To be sure, it is observed that the simply applying repetitive electrical stimulation to the sensory neuron is adequate to cause a continuous decrease in the dimensions of the postsynaptic EPSP.

Even though the basis for habituation could be identified as a synaptic modification, the question where the synapse is modified is still unanswered. The possibilities need to be checked at that point. Following habituation, the first thing is that the presynaptic axon does not allow enough neurotransmitters to transfer or secondly the post-synaptic responsiveness decreases to the transmitter (it is possible that there are few receptors). The quanta, the discrete packets where the transmitter molecules are released, are believed as correlating with the contents of individual synaptic vesicles. Promoting analyses showed that after habituation, there are less

quanta released per action potential. The sensitivity from neurotransmitter to postsynaptic cell remains the same. That is to say, it is the presynaptic modification related to the habituation of the gill-withdrawal reflex.

Here the question is why the neurotransmitter discharges less than the previous one after applying continuous stimulation of the sensory nerve terminal. When we look at the circle of events observed as the action potential in the terminal with the flow of neurotransmitter, the critical step is the Ca^{+2} entrance into the terminal that is forming the link by the voltage-gated calcium channels. It seems that the channels in the nerve terminal of the sensory neuron behave increasingly and insistently less effectively following habituation.

3.7.3 Sensitization of the Gill-Withdrawal Reflex

Kandel and his colleagues applied an abbreviated electrical shock to the head of Aplysia to cause a respond to the gill-withdrawal reflex. The result of this test was an enlarged gill with-drawal in response to stimulation of the siphon. With the help of this method, they found out a site of plasticity indicating differences that correlate with the behavior. One more time, it is the modification of transmitter release in the sensory nerve terminal. The sensory axon terminal is sensitized by the neurotransmitter serotonin. The serotonin receptor on the sensory axon terminal is named as G-protein-coupled metabotropic receptor. The impulse of this receptor paves the way for the production of intracellular second messengers. For this Aplysia sensory nerve terminal case, this second messenger is cyclic AMP (cAMP) that was produced by the enzyme adenylyl cyclase from ATP. Additionally, this cAMP changes protein kinase A, and this enzyme attaches phosphate groups to different proteins. One of these proteins is the potassium channel, which is located in the nerve terminal and phosphorylation of the channel ends up it to close. This closing action of potassium channels in the axon terminal causes an extension in the duration of the presynaptic action potential. This eventuates more Ca^{+2} entrance through voltage-gated calcium channels during the action potential, which causes more quanta of neurotransmitter to be released.

This updated research claims that this simple story is incomplete. Together with presynaptic modifications, persistent sensitization is related to increased postsynaptic responses to the neurotransmitter released by the sensory nerve. This neurotransmitter is

named as glutamate and sensitization is partially explained by the transmission of new glutamate receptors to the synapse.

3.7.4 Associative Learning in Aplysia

It is discovered that Aplysia could also be classically conditioned in the 1980s (Mark, 2001). It is the same method used as the measured response of the withdrawal of the gill. The strong shock to the tail was unconditioned-stimulus (US) and the stimulation of the siphon did not cause much response. It showed that if stimulation of the tail was shared with stimulation of the siphon, the following response to siphon stimulation alone was bigger than what could be calculated for by sensitization. Just like experiments of Pavlov, the timing was critical. Conditioning took place only if the conditioned-stimulus (CS) is proceeded the tail by $\leq$0.5 second.

One more time, a censorious modification is observed at the synapse between the sensory and the motor neuron. In order to understand the reason, the relation of CS-US pairing needs to be understood. The arrival of an action potential in the sensory axon terminal is represented as CS at the cellular level and the release of serotonin represents the US. And at the molecular level, the influx of Ca^{+2} represents CS and the G-protein coupled activation of the enzyme adenylyl cyclase in the terminal represents the US.

Remember that adenylyl cyclase creates cAMP. It means that if there were more cAMP, there would be more activation of protein kinase A, more phosphorylation of potassium channels and consequently the release of more transmitter molecules. Therefore, for the case of classical conditioning of the gill withdrawal reflex, adenylyl cyclase may perform as a detector of CS-US coincidence. By following this idea, learning happens when a presynaptic Ca^{+2} pulse coincides with the G-protein coupled activation of adenylyl cyclase that stimulates the producing of a lot of cAMP. Thus, when potassium channels are phosphorylated and neurotransmitter release is enhanced, memory occurs.

Yuriv Pershin and Massimilano diVentra described an artificial synapse as a synapse that remembers its history and it should be plastic according to the pre-synaptic and post-synaptic neuronal activity (Di Ventra-Pershin, 2012). As it has been mentioned, associative memory means any learning process in which a new response becomes associated with a particular stimulus (Silvia, 2009). They built a neural

network shown in Figure 3.19 for this type of associative memory system as in Kendel's experiments.

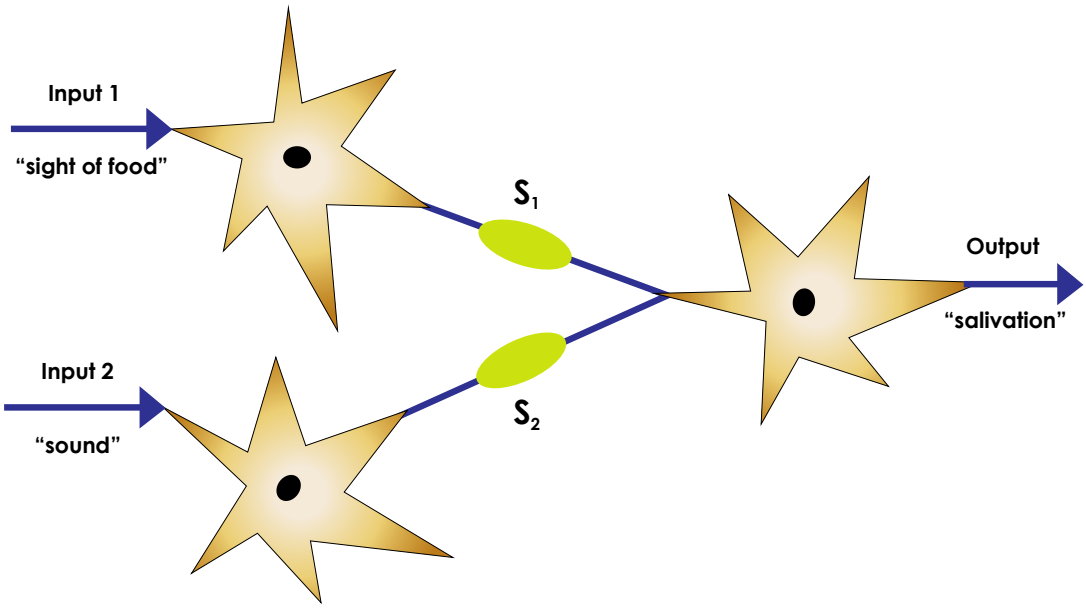

Figure 3.19 The model of Kendel's experiment

In their model, two neurons used for input of the system are connected a neuron used for output of the system. Here the input neurons are labeled as '1' and '2'. The neuron 1 is activated under a specific visual event such as 'sigh of food' and the neuron 2 is activated under an external auditory event such as particular ring sound. For instance, when a dog sees the food, salivation is observed. In Pavlov's experiment, for a certain moment of time the dog hears the ring sound with the sight of food at the same time. This event is repeated for a moment of time by the experimenter. Then only sound without the sight of food is enough to begin the salivation. This experiment proves the famous Hebbian rule stating that 'neurons that fire together wire together'. Their results are given in Figure 3.20.

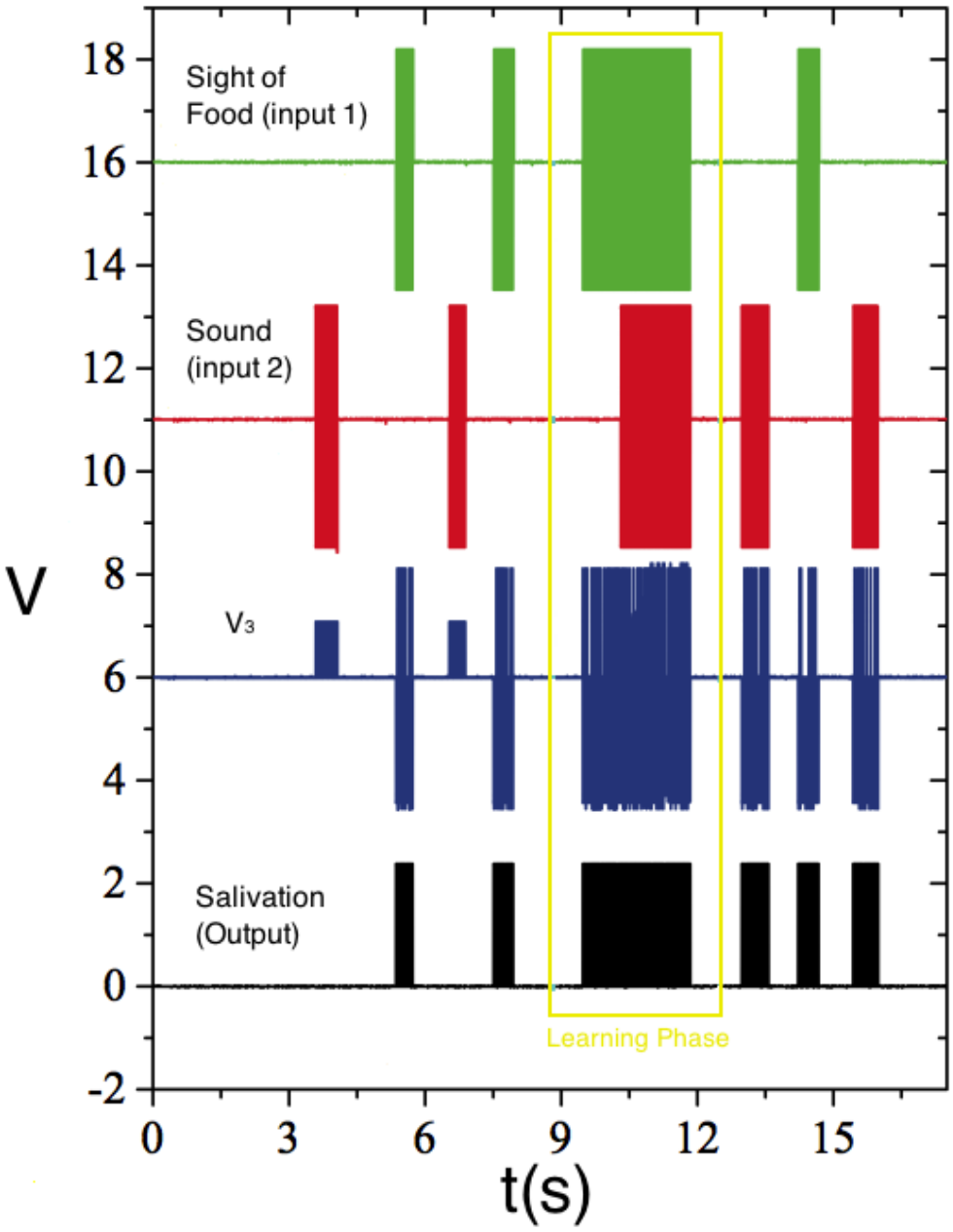

Figure 3.20: Input 1, input 2 and the output(Pershin, 2010)

The input 1, sight of food, and the input 2, sound, as shown in Figure 3.20 are applied to their memristor. The output signal is named as the salivation. Firstly they started with a strong first state and weak second state. The strong first state means that the first memristor has low resistance state and the weak second state means that the second memristor has high resistance state. For t<9s, they applied signals to the neuron 1 and 2 separately. Salivation is observed when neuron 1 is activated but it is not observed when neuron 2 is activated. In their model neuron 1 exceeded the threshold, but neuron 2 did not. For 9s<t<11s, they applied stimulus voltages simultaneously to

neuron 1 and neuron 2. These pulses were uncorrelated but sometimes they did overlap. The neuron 3, the salivation neuron, produce back-propagating pulses and these pulses did overlap with forward propagating pulses from the neuron 2. It causes a high voltage across the second memristor. With this voltage, the second memristor change its state from high-resistance state to low resistance state. It occurs if the inputs are correlated. This transition can be seen in Figure 3.21, V_3, as a growth of certain pulses(Pershin, 2010). It occurs in the time interval from 10,25s to 11s and it can be seen in Figure 3.21 in detail.

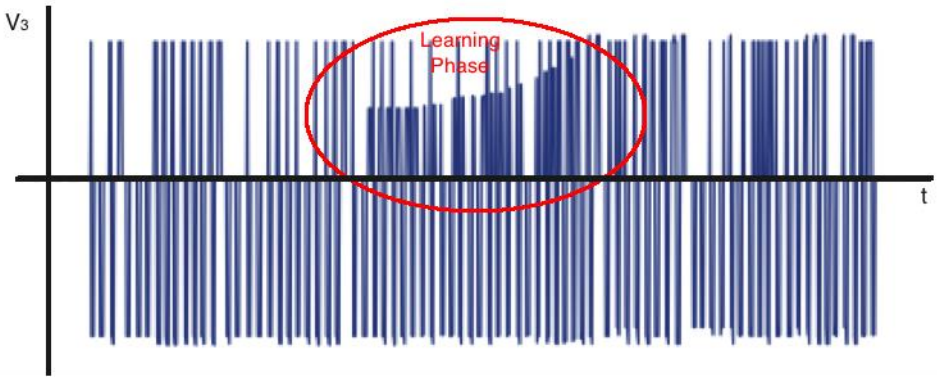

Figure 3.21 Detailed representation of the output. The learning phase is now noticeable.

For t>11s, neuron 1 or neuron 2 can trigger the neuron 3 alone. It means that salivation can be triggered by neuron 1 or neuron 2. Firing of any input neuron can trigger the firing of the output neuron. It also means that the associative memory is achieved as it has been mentioned above.

3.7.5 Amoeba Learning

Yuriv Pershin and Massimilano diVentra described an artificial synapse as a synapse that remembers its past history and it should be plastic according to the pre-synaptic and post-synaptic neuronal activity (Di Ventra-Pershin, 2010). Amoebalike cell *Physarum Polycephalum* was exposed to some periodic environmental changes. In the real world, it has been observed that these kinds of cells learn and adapt their behavior according to these environmental changes. They have adapted to the next coming stimulus by protecting themselves. The researchers have modeled this behavior by using a LC contour shown in Figure 3.23 and a memristor and they have used a train of

voltage pulsed to mimic the environmental changes. They connected the capacitor and the memristor in parallel and aimed to use the internal state of the memristor as an information-storing element about the past. They use the model of voltage-controlled memristor. The resistance of memristor can be M_1 , M_2 or the value of between these. In the model, M increases when the number of periodic stimuli increases. It is thought as a result of learning. The memristance M changes with

$$\frac{dM}{dt} = f(V_C)[\theta(V_c)\theta(M - M_1) + \theta(-V_c)\theta(M_2 - M_1)] \tag{3.42}$$

where

$$f(V) = -\beta V + 0.5(\beta - \alpha)(|V + V_T| - |V - V_T|). \tag{3.43}$$

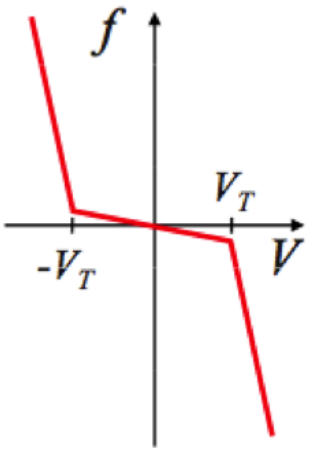

Figure 3.22: The characteristic function ‘f’ for the change of memristance vs. voltage loci (Pershin, 2010).

The change of memristance is described by a function of $f(V_C)$ and the applied voltage is V_C. Here θ is the step function. They assumed that $f(V_C)$ has several linear segments as shown in Figure 3.22. Here V_T is the threshold voltage and the memristor learns faster and slower when $|V_C| > V_T$ and $|V_C| < V_T$, respectively.

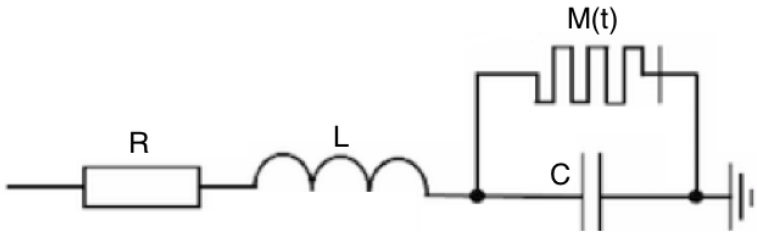

Figure 3.23: The circuit for the amoeba learning operation(Pershin, 2009)

The response of this circuit is given as

$$V_c + L\dot{I} + IR = V(t) \tag{3.44}$$

$$C\dot{V}_c + \frac{V_c}{M} = I \tag{3.45}$$

V_C is the voltage on the capacitor, I is the total current and V(t) is the applied voltage. They solved these equations numerically with Equation 3.42 and the results as shown in Figure 3.24.

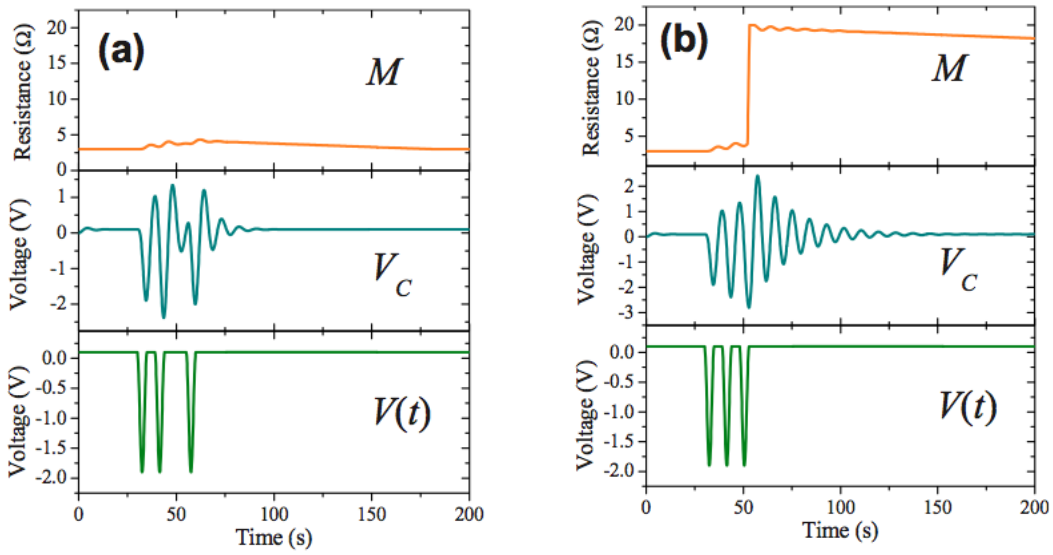

Figure 3.24: The applied aperiodic voltage pulses and the change of the memristance. The memristance change is not remarkable (a). The applied periodic voltage pulses and the change of memristance. The changed memristor resistance (b) (Pershin, 2009).

As it is seen from the model, the learning means the changing of the resistance of the memristor and it has been observed under the periodic voltage pulses. In Figure 3.24a, aperiodic voltage pulses do not change the memristance. When the periodic pulses are applied, the memristance is changed and it is seen from the Figure 3.24b. Unlike the periodic voltage pulses, the resistance may not reach the state that is accepted as a learning state about 20Ω under the periodic voltage pulses.

If the applied voltage is chosen as type of *sinusoidal* , (the duration is 35s) the memristance, the voltage on the capacitor and the current are shown as in Figure 3.25.

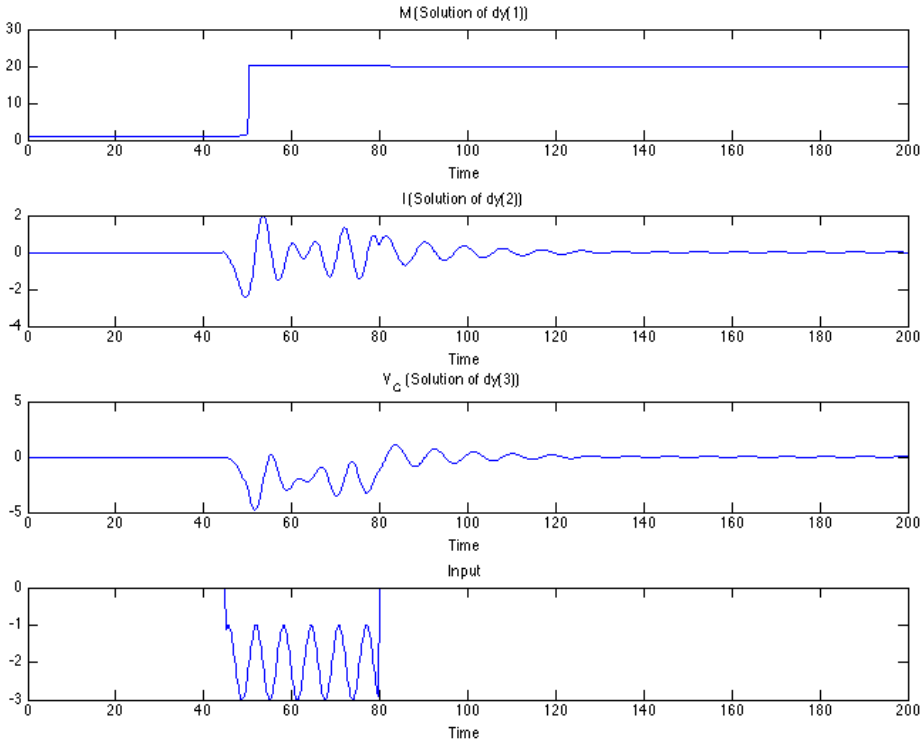

Figure 3.25. The memristance (dy_1) after the input voltage is applied, the current(dy_2) and the voltage of the capacitor(dy_3)

The applied voltage changes the memristance valu. If the applied voltage is chosen as shown in Figure 3.26, the memristance is changed to 20Ω.

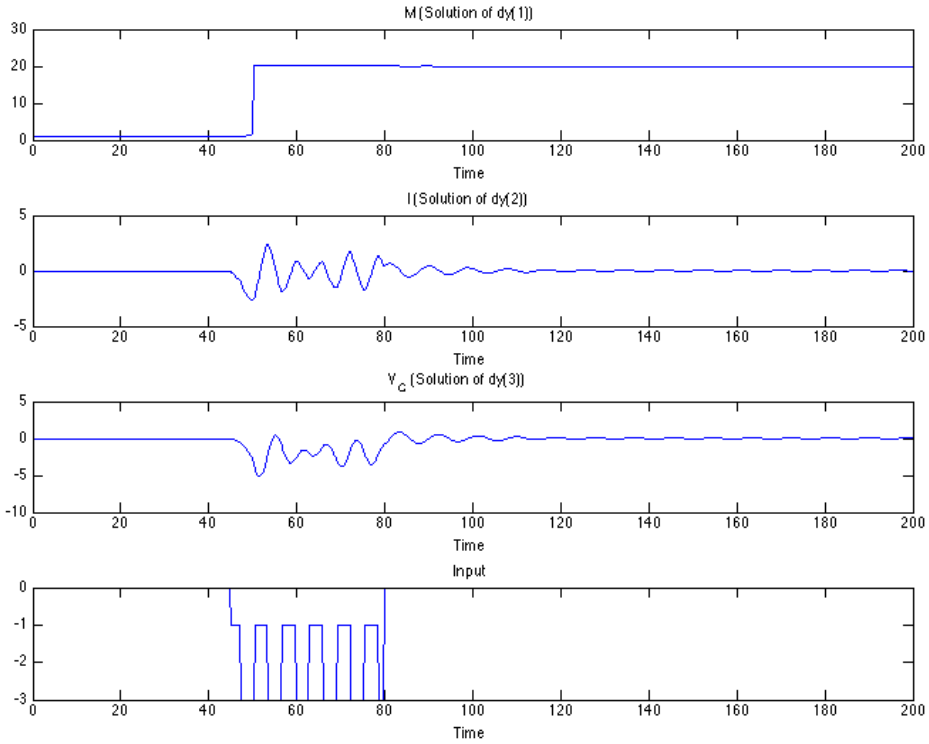

Figure 3.26. The memristance (dy_1) after the input voltage is applied, the current(dy_2) and the voltage of the capacitor(dy_3)

If the applied voltage is chosen as shown in Figure 3.27, the memristance is changed to 20Ω but it is not a stable value. It decreases again to 3Ω. It means that the learning phase does not occur.

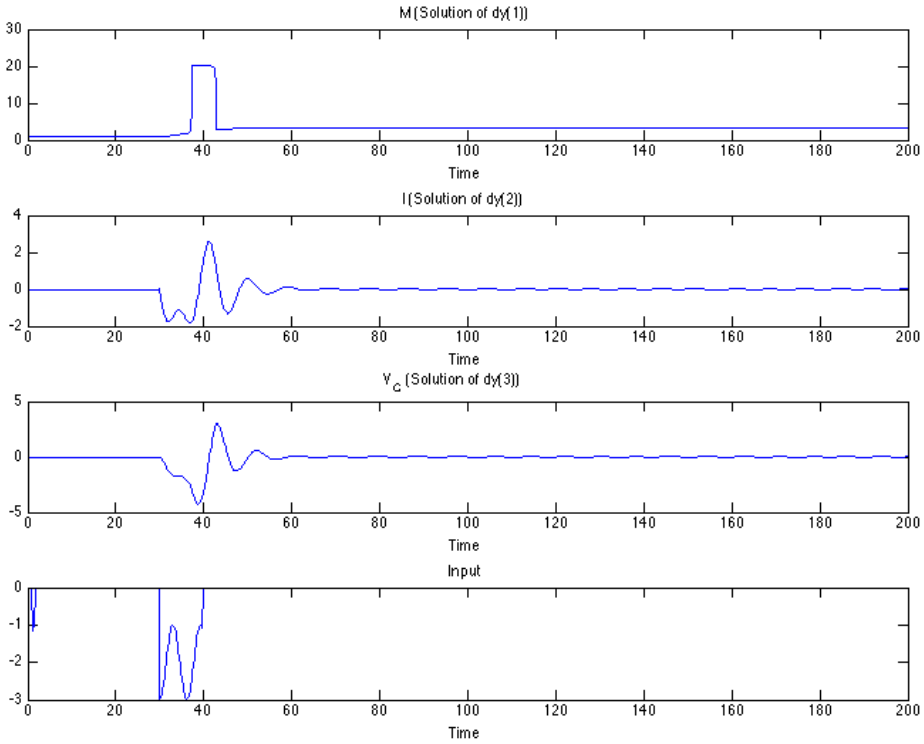

Figure 3.27. The memristance (dy_1) after the input voltage is applied, the current(dy_2) and the voltage of the capacitor(dy_3)

3.8 Memristor as a Biological Synapse

Sung Hyun *et.al*, experimentally exhibited a nanoscale silicon-based memristor device (Sung, et al. 2009). In neuromorphic circuits where high-effective computing is required, memristors can be used as synapses because of their abilities of high-connectivity (Yang, et al. 2013). In a biological system such as a mammalian cortex, neurons exhibit highly parallel processing. They showed an experiment, which implements synaptic functions in nanoscale silicon-based memristors. Their crossbar synapse network offers a computational system that corresponds to biological systems.

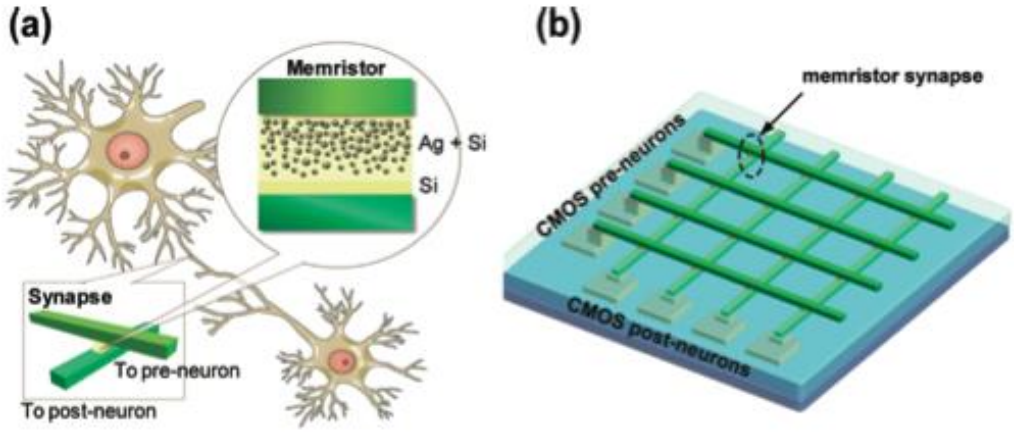

Figure 3.28: Memristor as a biological synapse (a) and memristor crossbar array (b)

They made their memristors cosputtered Ag and Si active layers. Their mixture of Ag and Si presents high conductivity if the formation is Ag-rich or if the formation is Ag-poor, it presents low conductivity. In Figure 3.29 (Yang, 2013), they showed that the measure current i(t) and the applied voltage across the terminals of memristor, v(t). They compared the experimental results with the HP model of memristors. The orange lines show the simple memristor circuit model. The blue lines are the measured results. The current for this model is described as

$$i(t) = \frac{1}{R_{on}w(t) + R_{off}\big(1 - w(t)\big)}v(t) \tag{3.46}$$

where w(t) has the value between 0 and 1.

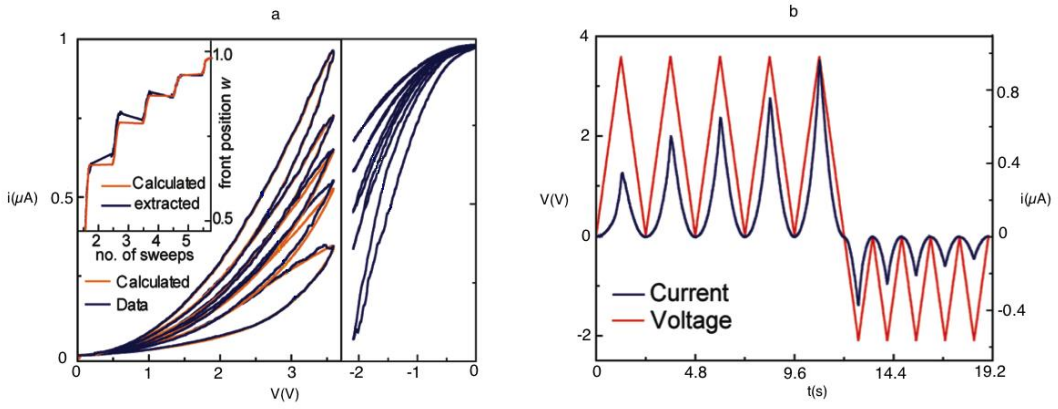

Figure 3.29 Experimental results compared to theoretical results(Yang, 2013)

The applied voltage V(t) is shown in Figure 3.29. When this applied voltage is positive, Ag ions are transferred to Ag-poor region. For this stage ‘w’ increases. When this applied voltage is negative, Ag ions are transferred to Ag-rich region. For this stage w decreases. The lowest and highest resistances are indicated as R_{off} and R_{on}, respectively. The threshold voltage is the minimum voltage value required to move ions to the other resistance area. In this work, the threshold voltage amplitude that is required to drive Ag ions to Si ions side is 2,2V. Below this amplitude, the memristor resistance remains stable.

They also applied some positive potentiating and negative depressing pulses. This device conductance after these pulses can be increased or decreased. They measured the conductance by applying a read voltage that is under the threshold voltage value. The read voltage must be smaller than the threshold voltage because the memristance should not be changed by this voltage value. This read voltage for this model is 1V. They then plotted this current versus pulse number and it is shown in Figure 3.30. The blue and red represent the positive pulses and negative pulses, respectively. It is clarified that the longer positive potentiating pulse increases the memristor conductance and vice versa. The applied positive and negative pulses (in figure b) change the conductance (shown green) positively and negatively, respectively.

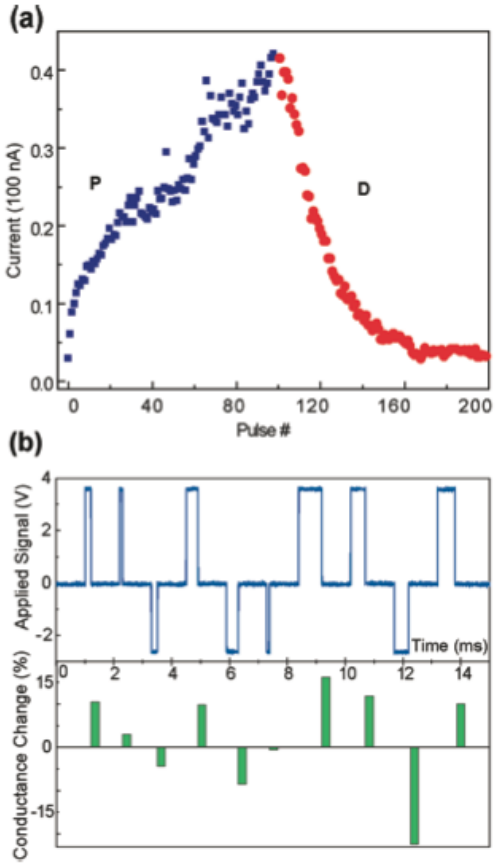

Figure 3.30. The applied positive and negative pulses (a) and the applied pulses(blue) and conductance changes(green) (Yang, 2013)

Unlike the work Nanoscale Device as Synapse in Neuromorphic System, Short-Term Plasticity and Long-Term Potentiating in single inorganic synapse presents an inorganic synapse that does not require any applied negative voltage to decrease the conductance (Takeo, et al. 2011). It is a very important property because biological synapses do not require that negative voltage pulse to decrease their weights. Ohno, et al. discovered that the Ag_2S inorganic synapse implements the biological facts, short-term plasticity and long-term potentiation. The conductance of this inorganic synapse is increased by Ag ions, but their work has a drawback. It is time-dependence. As it has been mentioned, the biological synapse may lose its efficiency over time, but this phenomenon is not observed for this Ag_2S inorganic synapse.

They applied input pulse with amplitude of 80mV. Its time width is 0,5s. For the STP, the time repetition intervals are 20s and for the LTP they are 2s. Also, the higher conductance is defined as 77,5μS.

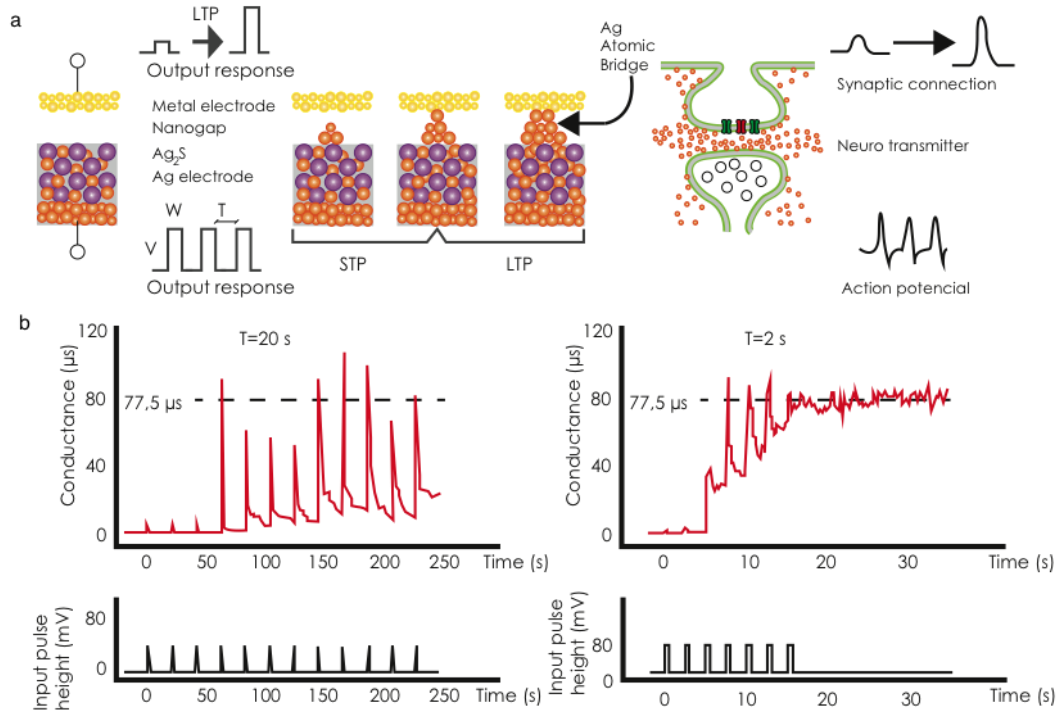

Figure 3.31. Physical representation of STP and LTP (a), conductance is changed by the applied voltage pulses (b).(Takeo, 2011)

The biological synapse formation and Ag_2S inorganic synapse formation is given in Figure 3.31a. The gates on the biological synapses are modeled with Ag atomic bridges. LTP requires new ion-channels formations for the biological synapses and this is modeled with the bridges in this inorganic synapse with pulses, intervals of 2s. The LTP is shown in Figure 3.31b. LTP is presented as the conductance changing of the inorganic synapse (Kuzum, et al. 2013). After pulses of 2s intervals are applied, the conductance level reaches 77,5µS and remains constant. This is the same characteristic of the biological LTP on the synapses and it is thought as learning. The STP is obtained with pulses, intervals of 20s. It is easily noticed that the conductance level does not reach the LTP level, 77,5µS and the learning process does not occur.

3.8.1 Forgetting Curves

In 1885, Hermann Ebbinghaus hypothesized that the nature of forgetting, generally known as forgetting curves (Hu et al. 2013). It shows the decline of memory retention in time and indicates that information is lost when there is no attempt to retain

it. If the memory is strong it means that the person is able to recall it for the longer period of time. He formulated this curve as

$$R = e^{-t/S} \tag{3.47}$$

where R is memory retention, S is the relative strength of memory and t is time.

Hu *et al.* emulated this curve by using NiO based memristor. After the application of electrical pulses, this memristor conductance decreases. In this work, the conductance corresponds to the memory stimulation or learning/forgetting events. They give the Ebbinghaus formulation in a more quantitative expression as

$$P = \exp(-(t/\tau)^{\beta}) \tag{3.48}$$

The stimulation parameters that emulate human memory loss behavior determine the decrease in conductance, which is similar to the memory. They have compared their results with Bi and Poo's results (Bi-Poo, 1998). Their result is very similar to that reference shown below. Figure 3.32 shows the memory loss defined with Equation 3.48 with relaxation time τ of 37s and β of 0,3. The circles refer to results of 'Bi and Poo'. The red line is the experimental result of NiO-based memristor. In Figure 3.31, they use $\tau = 68s$ and $\beta = 0{,}31$ and with these values, they showed that the decay of $\Delta G(t)/\Delta G_0$ is the analogue of the first graph memory loss in human brain where $\Delta G(t)$ is the conductance at the time t and ΔG_0 is the conductance of measured immediately after stimulation shown in Figure 3.33. The blue line is the experimental result of NiO-based memristor. As a conclusion, the forgetting curve is emulated with NiO-based memristor successfully.

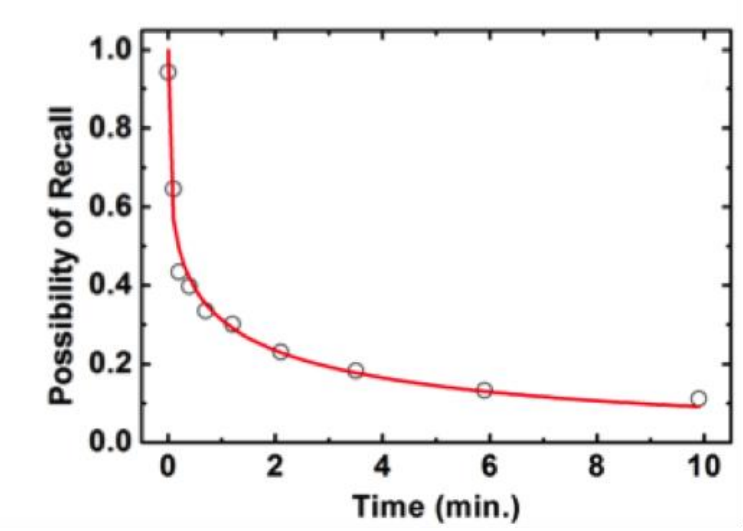

Figure 3.32 The memory recall possibility vs. time.(Hu S. 2013)

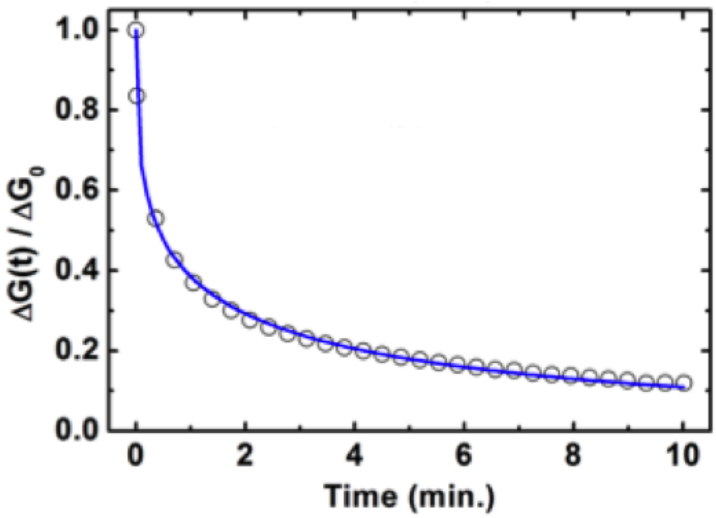

Figure 3.33 The change of conductance ratio vs. time(Hu S. 2013)

CHAPTER 4

THE MEMRISTIVE STORAGE SYSTEM

4.1 Memristive Storage for Images

According to HP, 100TB memristor hard-drives will be available for the commercial use of the personal computers in 2018. Memristors will be the main components of these types of devices. Bearing in mind that some researchers focus on that system. In 2012 XiaoFang et al. presented a memristive storage system for the gray-scale binary images and colorful images (XiaoFang *et. al*., 2012). First, they used MATLAB Simulink platform for the HP Memristor Model. In this model, their memristor is driven by $V = 1.2sin2\pi$. Their design is given in Figure 4.1.

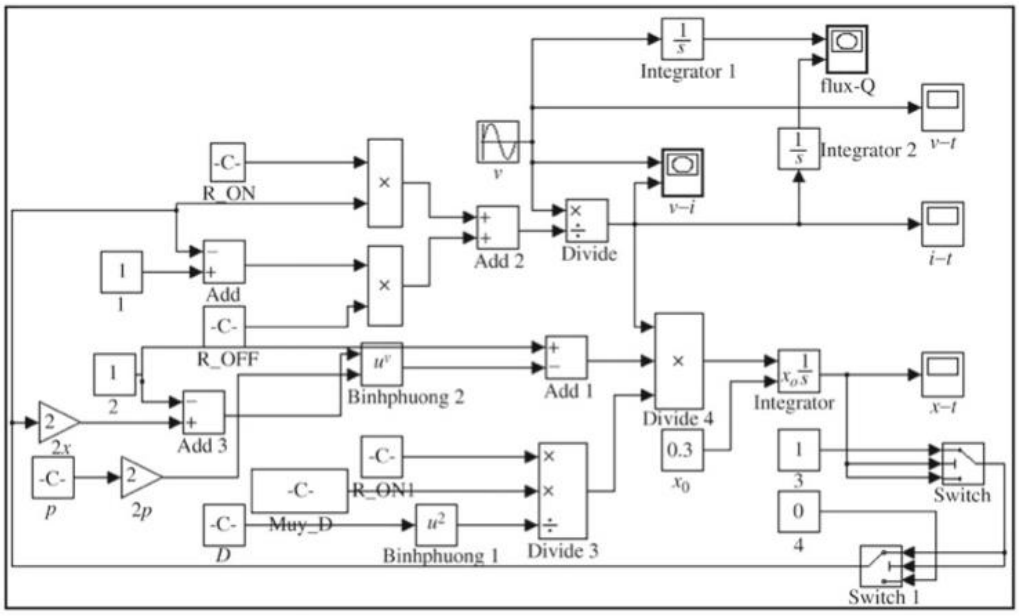

Figure 4.1 Memristor Simulink Model (XiaoFang *et. al*., 2012)

They applied different voltage pulses to their Memristor Simulink Model. In Figure 4.2 they applied a voltage pulse with height of 0.5V and weight of 2s. They showed that the memristance decreases more when the voltage pulse of 0.6V is applied.

They also applied a voltage pulse with height of 0.6V and weight of 2s. These voltage pulses are the same heights but different weights.

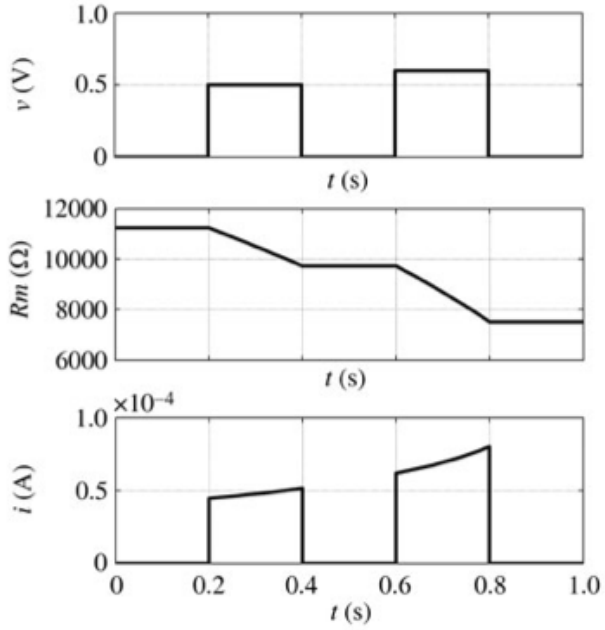

Figure 4.2. Different height voltage pulses, memristance values and currents.

In Figure 4.2(XiaoFang *et. al.*, 2012) they applied a series of positive and negative voltage pulses with identical amplitude 0.6V but different durations (0.1s and 0.2s). The positive voltage pulses decrease the memristance and the negative pulses increases the memristance shown in Figure 4.3. To return the memristance to its original state, a voltage pulse must be applied with the same amplitude and duration but opposite polarity.

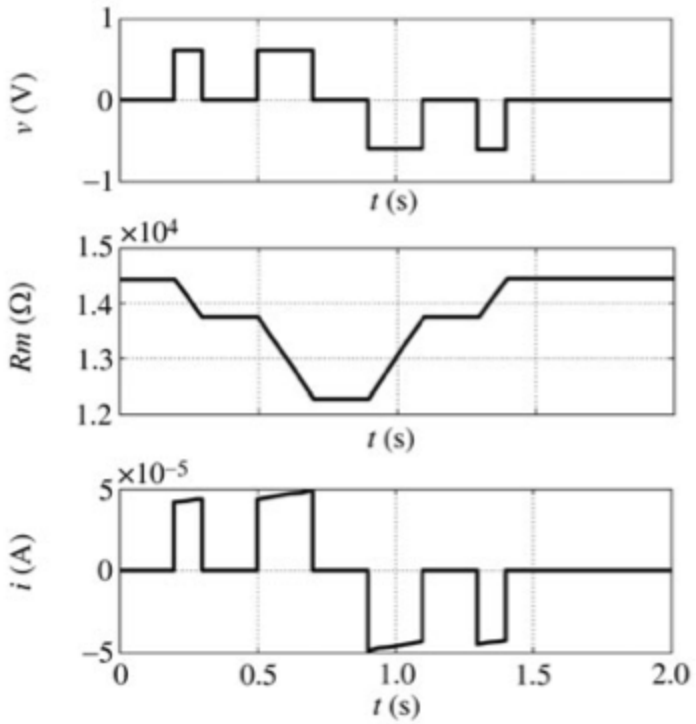

Figure 4.3. Different weight voltage pulses, memristance and current. (XiaoFang, 2012)

Some binary images are stored on the memristor crossbar array in their model. A memristor crossbar array composed of nanowires (because memristor is a nanoscale device), voltage converters and MUX circuit elements and memristors shown in Figure 4.4. Memristors are used on the crossbar points to connect the nanowires. They design a read/write control circuit to measure the memristance value. Different memristance values correspond to the different color tones of the images. They used MUX circuit elements to select the memristor in reading or writing operations. The voltage is applied by the voltage converter to intended memristors to achieve the storage. Their system measures the current flowing through the memristor. The read circuit compares the read current with the threshold value to determine the gray-scale tone of the image.

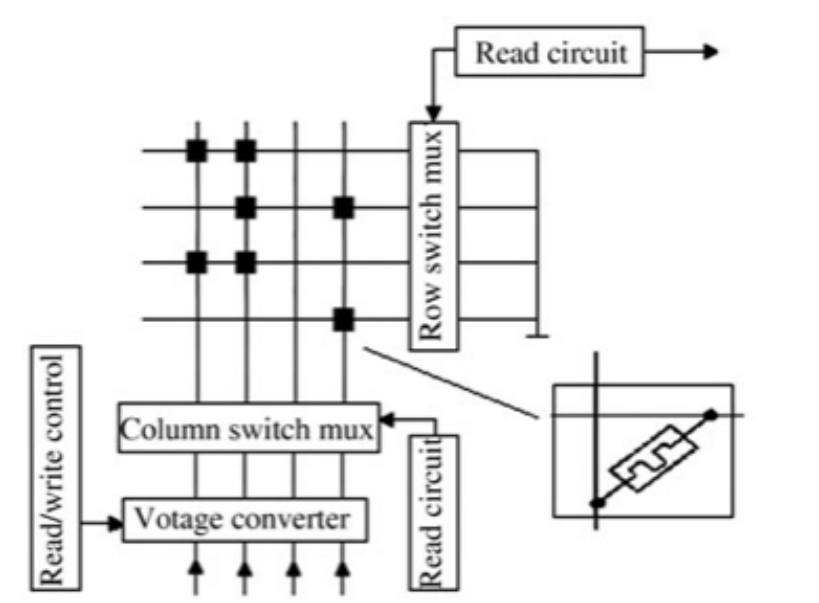

Figure 4.4. Memristive crossbar array storage system(XiaoFang, 2012)

They use 10x10 memristive crossbar array to store some binary images. Images are stored and then read successfully by the read/write circuits. The stored images and read images are shown in Figure 4.5a and Figure 4.5b, respectively.

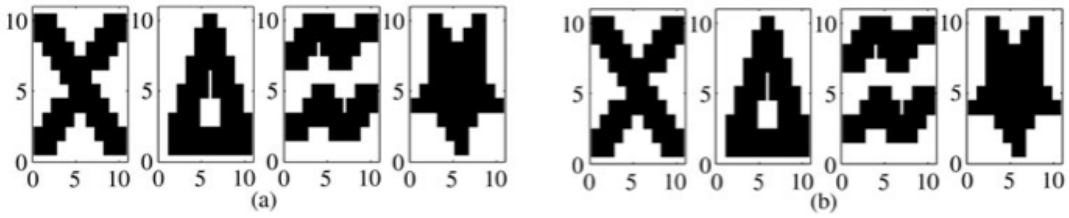

Figure 4.5. Stored images(a) and read images(b) (XiaoFang, 2012)

They then used different threshold values correspond to different gray-scale image tones. The stored image and read image are shown in Figure 4.6a and Figure 4.6b, respectively.

Figure 4.6. Gray-Scale stored image (a) and read image (b) (XiaoFang, 2012)

They finally use RGB monitoring system to store and read colorful images. They also used 3D memristor crossbar array. The colorful stored images and read images are shown in Figure 4.7.

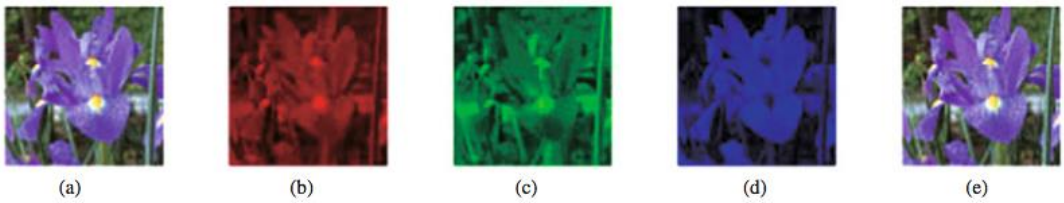

Figure 4.7. The colorful images(XiaoFang, 2012)

4.2 Memristive Crossbar Array Design for Binary Images

Due to the characteristic of a memristor, a memristor keeps its memory alive even if the power supply of the memristor is shut down (Chua, 1971). It shows a different resistance according to the current that passes through it or the flux-linkage on it. The high resistance value and the low resistance value have been described. At this point, it can be thought that the binary system for the computer language can be a basis for the memristive memory devices. As it is known, the binary system consists of 0 and 1. The similarity between the memristor model and the binary language system is that the high resistance value of the memristor can be thought as ‘1’ and the low resistance value can be thought as ‘0’. Aim of this chapter is to explain how to combine and

design a memristive memory system and then to write the data and read it carefully. As it can be understood from the HP memristor model (Strukov, et al. 2008), the current is very small and here it is important to design a system that should be very sensitive to this small current. Due to the fact that the memristor current is very small, the applied voltage to the memristor is very important because the data can be lost permanently. R. Stanley Williams describes how to constitute a memristive crossbar array (Williams, 2008). Hu, Duan et.al. and their groups have made some works, some of which are related to the memristive crossbar array applications (XiaoFang et al. 2012). In this chapter, the memristive crossbar array storage device has been designed and a binary image data has been stored to this device. This process is named as the 'Write Process'. Then the data, which is written to this system, has been read. This process is named as Read Process. At this reading process, a current threshold has been used to read the data sensitively. This threshold is very important to read the data because if a current which is higher or lower than the threshold is applied to the system, all the data might be lost or the device might be damaged.

4.2.1. The Device

The memristive storage system consists of MUX circuit elements, nanowires, voltage pulse sources and a voltage converter as shown in Figure 4.8. (XiaoFang, 2012)

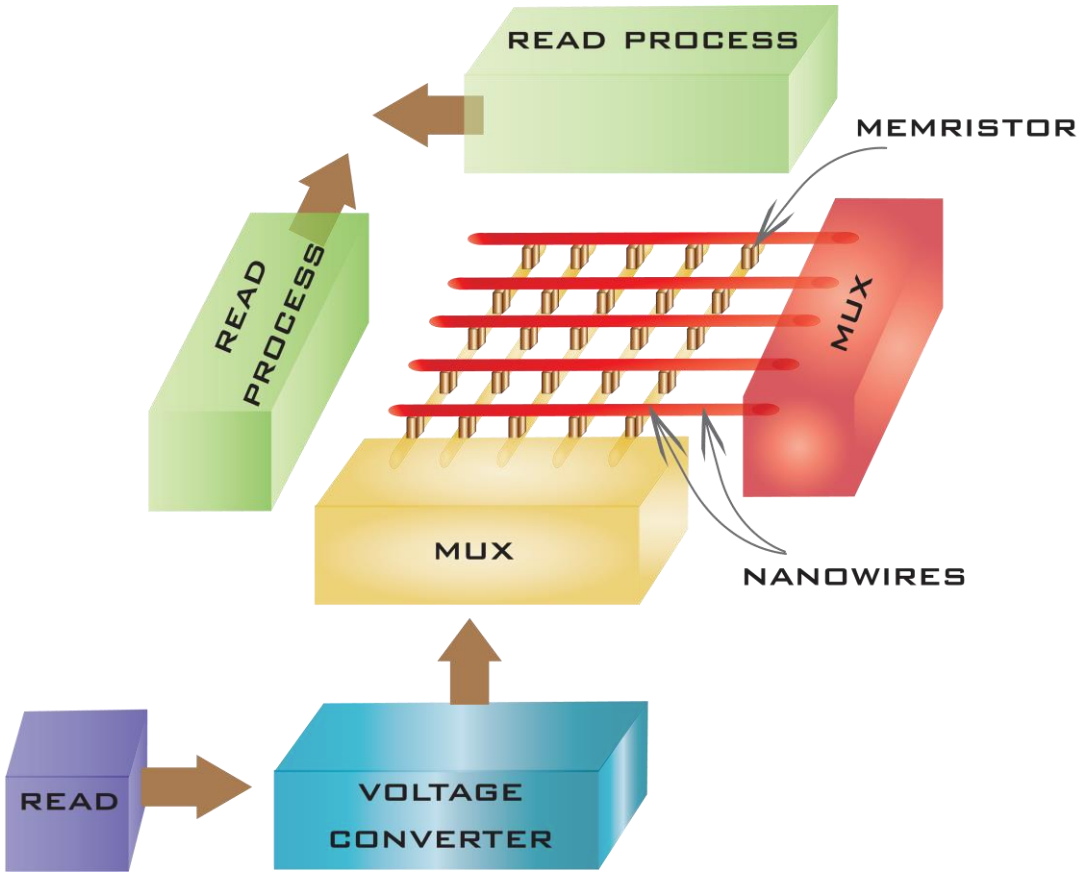

Figure 4.8: The storage system

4.2.2. The Write Process

In this process, every memristor is driven by a sinusoidal voltage source to write data. It is

$$V = Asin(2\pi ft) \tag{4.1}$$

All the memristors obey the $\varphi - q$ characteristics given as

$$q = \varphi + \frac{1}{3}\varphi^3 \tag{4.2}$$

The flux of a memristor can be found as

$$V = \frac{d\varphi}{dt} \Longrightarrow \varphi = \int_0^t V(t')dt' = \int_0^t \sin(1.2t) = -0.83(\cos(1.2t) - 1) \tag{4.3}$$

and the charge on the memristor from Equation 4.2

$$q = 0.83(1 - \cos(1.2t))\{1 + \frac{1}{3}\left(\frac{1}{(1.2)^2}\right)(1 - \cos(1.2t))^2\} \tag{4.4}$$

and the current through the memristor is

$$i(t) = \frac{dq}{dt} = [1 + \frac{1}{(1.2)^2}(1 - \cos(1.2t))^2]\sin(1.2t)$$

$$i(t) = [1 + 0.68(1 - \cos(1.2t))^2]\sin(1.2t) \tag{4.5}$$

To drive all the memristors simultaneously, mux circuit elements have been used. To write any data to the system, it is also important to know whether these memristors have been used before or not. At this point, a small DC voltage named as 'Checking Voltage' is applied to every memristor in the system. The value of this checking voltage pulse is 0.2V with width 0.1s for this system and it does not damage the data. This value changes the memristance value, but it is negligible. Once this voltage is applied to memristors, the fluxes of these memristors are changed, but they cannot exceed the threshold value that is responsible for keeping the data safe. Due to the fact that this applied voltage pulse does not cause any loss of data, it can be used as a checking voltage. After applying this checking voltage pulse, the flux of every memristors is read. If the flux exceeds the threshold (0.8Wb), it can be understood whether this memristor has a data or not. If this storage system is aimed to use for the first time, it also means that every memristor has no data so this checking process can be skipped. However if this system is not aimed to use for the first time, a negative

voltage pulse that is responsible to reset all data of memristors can be applied to the every memristor on the system. After all, it means that this storage system is ready to be used.

As it can be seen from the design Figure 4.8 and it has been mentioned, a memristor is a two-terminal circuit element. In the system, one of the terminals of each memristor is connected by the same MUX circuit element and the other one is connected by another MUX element. That is, if the nanowires come from the MUX1, which is connected to the terminal-one, the other terminal is connected to the terminal two by the nanowires, which come from the MUX2. Data can be written to the memristors by using these MUXs. As it has been mentioned, every memristor is driven by a voltage source $V = 1\sin(1.2t)$ to write the data to the memristor. The amplitude of this source is 1V. The applied frequency is 1,2Hz. To write a binary image to the memristors, every crossbar mentions a pixel for the binary image.

To determine which pixel has memory, the flux of the memristor should be checked. If the flux of a pixel is bigger than 0.8Wb, this pixel has data and it is called as a dark pixel. If the flux of the memristor is less than 0.8Wb, this pixel is an empty pixel as shown in Figure 4.9.

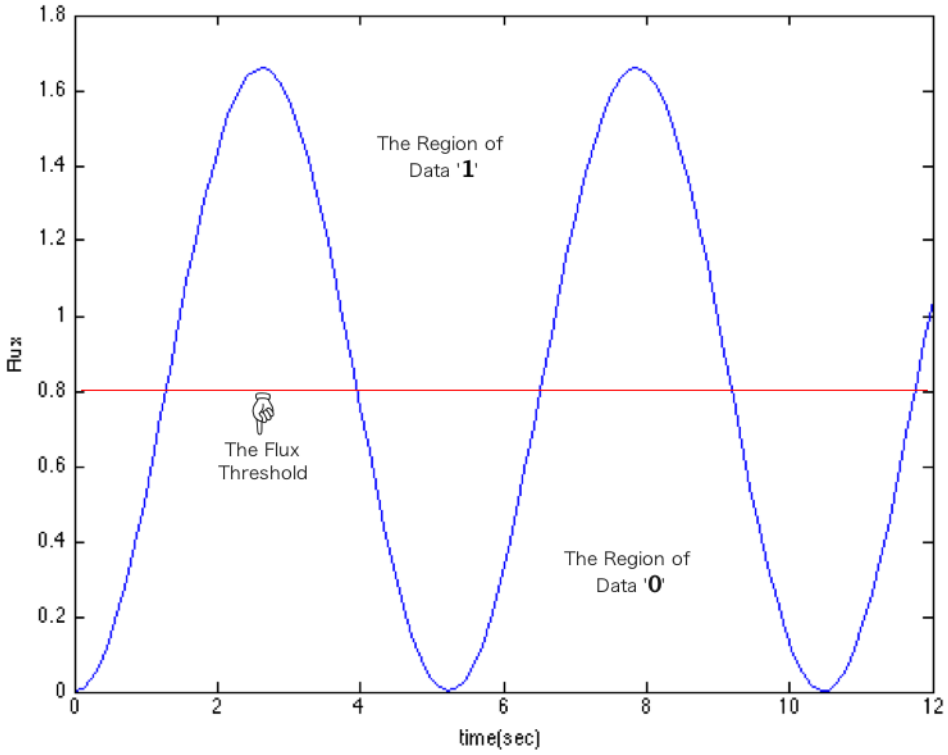

Figure 4.9 The flux threshold

On the crossbar, if a memristor corresponds to a dark pixel on the binary image, 1V pulse with width 1.5s will be applied by using MUXs to that memristor (write process). It also corresponds to ‘1’ in the binary computer language. If there is an empty pixel on the binary image, 0.5V pulse with width 0.1s is applied by using MUXs to that corresponding memristor. It also corresponds to the ‘0’ in the binary computer language. After the write voltages have been applied, they are all shut down. All the process means that the binary image is stored to the memristive storage device, to the crossbar.

Table 4.1: The dark and empty pixel voltage pulse values

The Dark Pixel	1V (1.5s)
The Empty Pixel	0.5V (0.1s)

4.2.3. The Read Process

All the data has now been stored to the memristive device. If the data is written correctly, it should be read. In the reading process a 0.2V is applied to every memristor. This applied voltage does not change the states of any memristors. It is named as ‘the Read Voltage’. After the read voltage is applied to every memristor, the flux value is read. For this memristive storage device, it is specified as 0.8W. It is named as ‘the Threshold Flux Value’. If the read circuit measures a flux that is bigger than this threshold, it means that this memristor has data on it. If the flux threshold of the corresponding memristor is bigger than 0.8Wb, then, this memristor represents a dark pixel of the binary image. If the flux threshold of the corresponding memristor is smaller than 0.8Wb, this memristor now represents an empty pixel of the binary image. With this step, it can be determined which memristor has data on it or not without losing any information.

In this thesis, a 12x60 crossbar array has been used to store a binary image. This storage device has 720 memristors. As it can be seen from the Figure 4.9, the threshold flux value is 0.8Wb. The read circuit determines the flux values and then decides which memristors have data. After this process, memristor that has flux bigger than 0.8Wb on the crossbar represents a dark pixel.

When the read process ends, the data that comes from the whole memristive system can be obtained. In order to obtain a binary image, every pixel represents a corresponding memristor. Some examples for this storage element are given below. In 12x60 crossbar memristive system, some of these letters are used to combine a word 'İZMİR'. For the letter case 12x12=144 memristors have been used to form a letter from I, Z, M, İ, R. For the word case, 12x60=720 memristors have been used to form İZMİR. Tables given below represent a memristor, which has data; here it is 1, on the memristor crossbar memory device.

4.3. The Word 'İZMİR'

These letters can be used together to form a word by changing the memristor number. For example it can be written 'İzmir' by combining letters İ,Z,M,İ,R. In order to do it the memristor number should be changed as given below. The new array has 12x60=720 memristors. In table 4.2 shows which memristors on the array will have a value of '1'

Table 4.2: The crossbar place of which memristor has data for the word 'İZMİR'

```
(3,6)=1;(3,7)=1;(4,6)=1;(4,7)=1;(5,6)=1;(5,7)=1;(6,6)=1;(6,7)=1;
(7,6)=1;(7,7)=1;(8,6)=1;(8,7)=1;(9,6)=1;(9,7)=1;(10,6)=1;(10,7)=1;
(3,15)=1;(3,16)=1;(3,17)=1;(3,18)=1;(3,19)=1;(3,20)=1;(3,21)=1;
(3,22)=1;(4,15)=1;(4,16)=1;(4,17)=1;(4,18)=1;(4,19)=1;(4,20)=1;
(4,21)=1;(4,22)=1;(5,21)=1;(5,22)=1;(6,19)=1;(6,20)=1;
(7,17)=1;(7,18)=1;(8,15)=1;(8,16)=1;
(9,15)=1;(9,16)=1;(9,17)=1;(9,18)=1;(9,19)=1;(9,20)=1;(9,21)=1;
(9,22)=1;(10,15)=1;(10,16)=1;(10,17)=1;(10,18)=1;(10,19)=1;
(10,20)=1;(10,21)=1;(10,22)=1;(3,27)=1;(3,28)=1;(3,33)=1;
(3,34)=1;(4,27)=1;(4,28)=1;(4,33)=1;(4,34)=1;(5,27)=1;(5,28)=1;
(5,29)=1;(5,32)=1;(5,33)=1;(5,34)=1;(6,27)=1;(6,28)=1;(6,29)=1;
(6,32)=1;(6,33)=1;(6,34)=1;(7,27)=1;(7,28)=1;(7,29)=1;(7,30)=1;
(7,31)=1;(7,32)=1;(7,33)=1;(7,34)=1;(8,27)=1;(8,28)=1;(8,30)=1;
(8,31)=1;(8,33)=1;(8,34)=1;(9,27)=1;(9,28)=1;(9,33)=1;(9,34)=1;
(10,27)=1;(10,28)=1;  (10,33)=1;(10,34)=1;
(2,42)=1;(2,43)=1;(4,42)=1;(4,43)=1;(5,42)=1;(5,43)=1;(6,42)=1
(6,43)=1;(7,42)=1;(7,43)=1;(8,42)=1;(8,43)=1;(9,42)=1;(9,43)=1;
(10,42)=1;(10,43)=1;(3,51)=1;(3,52)=1;(3,53)=1;(3,54)=1;(3,55)=1;
(3,56)=1;(3,57)=1;
(4,51)=1;(4,52)=1;(4,53)=1;(4,54)=1;(4,55)=1;(4,56)=1;(4,57)=1;
(4,58)=1;(5,51)=1;(5,52)=1;(5,58)=1;(6,51)=1;(6,52)=1;(6,58)=1;
(7,51)=1;(7,52)=1;(7,53)=1;(7,54)=1;(7,55)=1;(7,56)=1;(7,57)=1;
(7,58)=1;(8,51)=1;(8,52)=1;(8,53)=1;(8,54)=1;(9,51)=1;(9,52)=1;
(9,55)=1;(9,56)=1;(10,51)=1;(10,52)=1;(10,57)=1;(10,58)=1;
```

The obtained image from this 12x60 crossbar array is given by

Figure 4.10: The read word ‘İZMİR’

4.4 Edge Detection for Images

For the dynamics of a cellular neural network are governed by the differential equations given as

$$\frac{dx_{ij}}{dt} = -\gamma x_{ij} + \sum_{k,l \in N_{ij}} \left(a_{k,l} y_{kl} + b_{k,l} u_{kl}\right) + z_{ij} \tag{4.6}$$

where (i,j)∈{1,...,M}x{1,...,N}. N_{ij} is the r-neighborhood of cell C_{ij}, a_{kl}, b_{kl} and z_{ij} are the feedback, control and threshold template parameters, respectively. A=[a_{kl}] and B=[b_{kl}] are the feedback template and feed-forward template matrices, respectively (Chua *et al*., 2009). y_{ij} is the output. Chua describe the relationship between the output and the states x_{ij} of each cell via a piecewise-linear function. It is given as

$$y_{ij} = f(x_{ij}) = \frac{1}{2}\{|x_{ij} + 1| - |x_{ij} - 1|\} \tag{4.7}$$

The neighborhood radius of each cell is restricted to 1, assume that z_{ij} is the same for the whole network.

As we know, the time derivative of Equation 4.6,

$$\frac{dx_{ij}}{dt} = \frac{x_{ij}(t + \Delta t) - x_{ij}(t)}{\Delta t} \tag{4.8}$$

it is obtained as

$$\frac{x_{ij}(t+\Delta t)-x_{ij}(t)}{\Delta t}=-\gamma x_{ij}(t)+\sum_{k,l\in N_{ij}}\left(a_{k,l}y_{kl}(t)+b_{k,l}u_{kl}\right)+z_{ij} \tag{4.9}$$

For $\Delta t = 1$, it is obtained as

$$x_{ij}(t+1)-x_{ij}(t)=-\gamma x_{ij}(t)+\sum_{k,l\in N_{ij}}\left(a_{k,l}y_{kl}(t)+b_{k,l}u_{kl}\right)+z_{ij} \tag{4.10}$$

with $c = 1-\gamma$, the Equation 4.10 is formed as

$$x_{ij}(t+1)=cx_{ij}(t)+\sum_{k,l\in N_{ij}}\left(a_{k,l}y_{kl}(t)+b_{k,l}u_{kl}\right)+z_{ij} \tag{4.11}$$

By setting c=0 the discrete-time recursive equation is obtained as

$$x_{ij}(t+1)=\sum_{k,l\in N_{ij}}\left(a_{k,l}y_{kl}(t)+b_{k,l}u_{kl}\right)+z_{ij} \tag{4.12}$$

where t=0,1,2,..

With the Equation 4.12, Equation 4.7 is formed as

$$y_{ij}(t+1)=f\left(x_{ij}(t+1)\right)=f(\sum_{k,l\in N_{ij}}\left(a_{k,l}y_{kl}(t)+b_{k,l}u_{kl}\right)+z_{ij}) \tag{4.13}$$

For the memristive cellular automaton, the signal $z_{ij}(t)$ satisfies the equation

$$z_{ij}(t)=y_{ij}(t-T)-y_{ij}(t-2T+1) \tag{4.14}$$

where $y_{ij}(t-T)$ corresponds to a positive pulse and $y_{ij}(t-2T+1)$ corresponds to a negative pulse. The negative pulse is required to discharge to the memristor as it has been mentioned in Chapter 2 for the logical operations by memristors. The charge $q_{ij}(t)$ stored in the memristor during the period (nT, nT+Δt) is given by

$$\begin{aligned} q_{it}(nT+\Delta t) &= \sum_{k,l\in(-1,0,1)} a_{k,l}z_{i+k,j+l}(nT)+\Delta t \\ &= \sum_{k,l\in(-1,0,1)} a_{k,l}y_{i+k,j+l}\big((n-1)T\big)+\Delta t \end{aligned} \tag{4.15}$$

for 0<Δt<1. Here the charge stored by a positive current pulse is indicated by Δt. From the equations $y_{ij}(t) = V(t) = M\big(q(t)\big)I_p(t)$ and $V(t) = M\big(q(t)\big)I_p(t)$, the output is obtained as

$$y_{ij}(nT + \Delta t) = \tag{4.16}$$

$$= \begin{cases} M\left(q_{ij}(nT + \Delta t)\right) = M\left(\sum_{k,l\in(-1,0,1)} a_{k,l}y_{i+k,j+l}\big((n-1)T\big) + \Delta t\right), I_p > 0 \\ 0, \quad I_p < 0 \end{cases}$$

It is time to describe the rules for the edge detection operations. An edge is the intensity changings between the pixels of an image. The rule is as follows:

i- The new state of the cell will be 'black' if the total number of the black cells is equal to 6, 7 or 8.

ii- If the total number of black cells is equal to 0, 1, 2, 3, 4, 5, 9, the new state of the cell will be 'white'.

The rule of the edge detection is summarized in Table 4.3.

Table 4.3: The Edge Detection Rule

$\sum_{k=-1}^{1}\sum_{m=-1}^{1} y_{i+k,j+m}((n-1)T)$	9	8	7	6	5	4	3	2	1	0
New state of the center cell $y_{ij}(nT)$	0	1	1	1	0	0	0	0	0	0

where the y_{ij} has two states '0' and '1' ,which denotes white and black representation of the binary image. The rule implies that if the number of black pixels in the 3x3 blocks is 6, 7 or 8, that cell produces a black cell. This rule is shown in Figure 4.11 and Table 4.3.

Example of cell patterns	■■■ ■■■ ■■■	■■□ ■■■ ■■■	■□■ ■□■ ■■■	■□■ ■□■ ■□■	□□■ □■■ □■■	□■□ □■□ □■■	□□■ □□■ □■□	□□■ □□■ □□□	□□□ □□□ □□■	□□□ □□□ □□□
Number of black cells	**9**	**8**	**7**	**6**	**5**	**4**	**3**	**2**	**1**	**0**
New state for center cell	□	■	■	■	□	□	□	□	□	□

Figure 4.11: Example of neighborhood patterns for the edge detection rule

The memristance for the rule of the edge detection is given as follows:

$$M(q) = M_6(q) + M_7(q) + M_8(q) = \begin{cases} 0 & for\ q = 0,1,2,3,4,5,9 \\ 1 & for\ q = 6,7,8 \end{cases} \tag{4.17}$$

or by using the floor function

$$M(q) = u(floor(|q|) - 5) - u(floor(|q|) - 8). \tag{4.18}$$

The difference equation is given by

$$\begin{aligned} y_{ij}(nT + \Delta t) = u\left(floor\left|\sum_{k,l\in(-1,0,1)} a_{k,l}y_{i+k,j+l}\big((n-1)T\big) + \Delta t\right| - 5\right) \\ - u\left(floor\left|\sum_{k,l\in(-1,0,1)} a_{k,l}y_{i+k,j+l}\big((n-1)T\big) + \Delta t\right| - 8\right), \end{aligned} \tag{4.19}$$

where the weighting matrix A is given as

$$A = \begin{bmatrix} 1 & 1 & 1 \\ 1 & 1 & 1 \\ 1 & 1 & 1 \end{bmatrix} \tag{4.20}$$

Firstly, the image is transformed to the black-white image. Then the edge detection rule is applied to that black-white image. Two edge-detection operations are presented as examples. The first presented image is the original image. The second one is the

transformed black-white image. The last one is the edge-detected image.

Example 1:

Figure 4.12: The original image (a), the black-white image (b) and the edge-detected image (c).

In Figure 4.12, the first example is presented. Figure 4.12a, 4.12b, and 4.12c represent the original image, black-white image and edge-detected image, respectively.

Example 2:

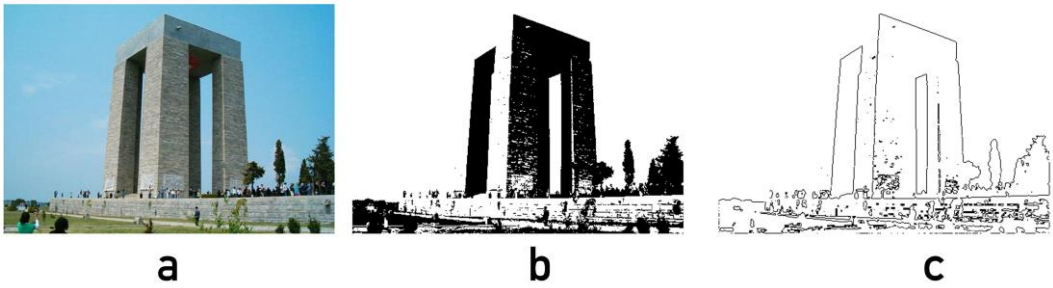

Figure 4.13. The original image (a), the black-white image (b) and the edge-detected image (c).

In Figure 4.13, the first example is presented. Figure 4.13a, 4.13b, and 4.13c represent the original image, black-white image and edge-detected image, respectively. The edges are detected by the memristor cellular automaton according to the rule of the edge-detection given in Table 4.3.

CHAPTER 5

CONCLUSION

In this thesis, the memristor theory is explained. The applications of memristors in different areas have been increasing since the physical implication of memristor by HP. All these researches carried out using these different applications show that the characteristics of the memristor are behaving closely the same as brain functions such as learning, memory storage and forgetting.

The learning activity in brain is the last product of increasing number of the receptor. Also, these numbers depend on the amount of the concentrations of Ca^{+2} ions in the neurons. If the pulse is adequate, the memristor changes its resistance from the certain rate to a different rate. This situation, which is observed for memristor, is closely the same as the Ca^{+2} ions in the neuron. Thus, there are some cases of memristors that are practiced physically have managed to implicate learning and forgetting functions of brain.

In addition to the physically practiced cases of memristors, Chua suggests that memristors are the elements that can be used as storage devices since they have a specific characteristic of resistance switching.

There are also other cases on primitives as they have a capacity of learning and acting strategies according to the situations they are in or the other creatures surrounding them as an action. These cases for primitives show that the actions of these primitives can be modelled by using memristor.

However, the rate of the resistance of the memristor is not stable. It depends on the applied voltage or applied current. The resistance value remains stable when the last applied voltage or current is shut down. By using this technique and also the MUX circuit elements, the “Memristor Crossbar Array” is designed to save and read data. A 12x60 memristor crossbar array has been used to design a crossbar system. Then a flux threshold level is determined. After all, a binary image ‘İZMİR’ has been saved and read successfully. Also, the edge detection system has been introduced by using memristor cellular automata and the edges of two images have been found according to the edge detection rule of this cellular automata.

REFERENCES

Bailey Craig H., and Eric R. Kandel, (1993). 'Structural changes accompanying memory storage.' *Annual review of physiology* 55.1: 39426.

Beatty Jackson, (1995). 'Principles of behavioral neuroscience'. Brown & Benchmark Publishers.

Bi Guo-qiang, and Mu-ming Poo, (1998). 'Synaptic modifications in cultured hippocampal neurons: dependence on spike timing, synaptic strength, and postsynaptic cell type.' *The Journal of neuroscience* 18.24: 10464-10472.

Chua L., (1971). 'Memristor-the missing circuit element.' *Circuit Theory, IEEE Transactions on*, *18*(5), 507-519.

Chua L., (2011). 'Resistance switching memories are memristors.' *Applied Physics A* 102.4: 765-783.

Chua L., (2013). 'Memristor, Hodgkin–Huxley, and Edge of Chaos.' *Nanotechnology* 24.38: 383001.

Chua L. Makoto Itoh(2009). Memristor Cellular Automata and Memristor Discrete-time Cellular neural networks, International Journal of Bifurcation and Chaos, Vol. 19, No. 11 (2009) 3605–3656

Caporale Natalia and Yang Dan, (2008). 'Spike timing-dependent plasticity: a Hebbian learning rule.' *Annu. Rev. Neuroscience.* 31: 25-46.

Harth E. M., Csermely T. J., Beek B., Lindsay R. D., (1970). 'Brain functions and neural dynamics.' *Journal of Theoretical Biology*, *26*(1), 93-120.

Hu S. G., Liu Y., Chen T. P., Liu Z., Yu Q., Deng L. J., Hosaka S., (2013). 'Emulating the Ebbinghaus forgetting curve of the human brain with a NiO-based memristor.' *Applied Physics Letters*, *103*(13), 133701.

Hu X., Duan S., Wang L., Liao X., (2012). 'Memristive crossbar array with applications in image processing. *Science China Information Sciences*, *55*(2), 461-472'.

Iu H. H. C., Fitch A. L., (2013). 'Development of Memristor Based Circuits (Vol. 82)'. World Scientific.

Izhikevich E. M., (2007). ‘Dynamical systems in neuroscience.’ MIT press.

Jo S. H., Chang T., Ebong I., Bhadviya B. B., Mazumder P., Lu W., (2010). ‘Nanoscale memristor device as synapse in neuromorphic systems.’ *Nano letters*, *10*(4), 1297-1301. ACS Publication.

Kandel Eric R., (2007) ‘In search of memory: The emergence of a new science of mind’. Norton & Company.

Kuzum Duygu, Shimeng Yu, and H. P. Wong, (2013). ‘Synaptic electronics: materials, devices and applications.’ *Nanotechnology* 24.38: 382001.

Mark F., W. C. Barry, and A. P. Michael, (2001) ‘Neuroscience: exploring the brain.’ *Maryland: Lippincott williams and wilkins*: 682-3.

Malenka Robert C., (1994). ‘Synaptic plasticity in the hippocampus: LTP and LTD.’ *Cell Press* 78.4: 535-538.

Ohno T., Hasegawa T., Tsuruoka T., Terabe K., Gimzewski J. K., Aono M., (2011). ‘Short-term plasticity and long-term potentiation mimicked in single inorganic synapses’. *Nature materials*, *10*(8), 591-595.

Pershin Yuriy V., Steven La Fontaine, and Massimiliano Di Ventra, (2009). ‘Memristive model of amoeba learning.’ *Physical Review E* 80.2: 021926.

Pershin Yuriy V., and Massimiliano Di Ventra, (2010) ‘Experimental demonstration of associative memory with memristive neural networks.’*Elsevier,* 23.7: 881-886.

Strukov D. B., Snider G. S., Stewart D. R., Williams R. S., (2008). ‘The missing memristor found’. *Nature*, *453*(7191), 80-83.

Snider Greg S. (2008) ‘Cortical computing with memristive nanodevices.’ *SciDAC Rev* 10: 58-65.

Snider Greg S., (2008). ‘Spike-timing-dependent learning in memristive nanodevices.’ *Nanoscale Architectures. IEEE International Symposium*.

Thomas Andy, (2013). ‘Memristor-based neural networks.’ *Journal of Physics D: Applied Physics* 46.9: 093001.

Williams R., (2008). ‘How we found the missing memristor.’ *Spectrum, IEEE* 45.12:28-35.